Other Applications, Including the Critical Care Setting

19

Pei-Ni Jone and Adel Younoszai

Abbreviations

2D	Two-dimensional
3D	Three-dimensional
CHD	Congenital heart disease
CHF	Congestive heart failure
DVI	Doppler velocity index
EOA	Effective orifice area
IE	Infective endocarditis
PPM	Patient-prosthesis mismatch
SVC	Superior vena cava
TAVR	Transcatheter aortic valve replacement
TEE	Transesophageal echocardiography
THV	Transcatheter heart valve
TTE	Transthoracic echocardiography
VTI	Velocity time integral

Key Learning Objectives

- Describe the echocardiographic manifestations of infective endocarditis (IE)
- Define the role of transesophageal echocardiography (TEE) for the evaluation of IE, and its use compared to transthoracic echocardiography
- Outline the key echocardiographic characteristics of intracardiac thrombus, and how they are evaluated by TEE
- Distinguish the key differences between mechanical and bioprosthetic valves
- Review the methodology for echocardiographic evaluation of mechanical valves

Electronic Supplementary Material The online version of this chapter (https://doi.org/10.1007/978-3-030-57193-1_19) contains supplementary material, which is available to authorized users.

P.-N. Jone (✉) · A. Younoszai
Pediatric Cardiology, Children's Hospital Colorado, University of Colorado School of Medicine, Aurora, CO, USA
e-mail: pei-ni.jone@childrenscolorado.org; adel.younoszai@childrenscolorado.org

Introduction

The vast majority of transesophageal echocardiography (TEE) studies performed in pediatric patients with acquired or congenital heart disease (CHD) is generally performed during operative or interventional procedures. The same holds true for a large proportion of adult patients with CHD. Nonetheless, there are other settings in which TEE can prove beneficial in such patients. This chapter focuses on other applications of TEE in pediatric and adult patients with and without CHD, including the critical care setting. Frequently, TEE is used in critically ill patients who have poor acoustic windows. We will discuss the most common indications for TEE in this setting, including evaluation for infective endocarditis, cardiac thrombi after CHD surgery, and prosthetic valves.

Infective Endocarditis

Infective endocarditis (IE) is a bacterial or fungal infection of the endocardium of the heart and great vessels, and usually occurs in the setting of a preexisting abnormality of the heart or great arteries [1]. It may occur in a normal heart during septicemia or as a consequence of infected indwelling central catheters [1]. Common organisms causing IE are *Streptococcus viridans* (30–40% of cases), *Staphylococcus aureus* (25–30%), and fungal agents (about 5%). The infectious process is highly invasive and can cause destruction of heart valves and surrounding tissue. It can lead to intramyocardial abscess, congestive heart failure (CHF) from valve regurgitation, systemic and pulmonary emboli, sepsis, arrhythmias, myocardial failure, and even death [2]. In the pediatric population, the frequency of infective endocarditis (IE) appears to be increasing [1] for several reasons: (1) increased survival in children with CHD, (2) greater use of central venous catheters, and (3) increased use of prosthetic material and valves. Pediatric patients without preexisting heart disease are also at increased risk for IE because of (1) increased survival rates for children with immune deficiencies, (2) long-term use of

P. C. Wong, W. C. Miller-Hance (eds.), *Transesophageal Echocardiography for Pediatric and Congenital Heart Disease*,
https://doi.org/10.1007/978-3-030-57193-1_19

Table 19.1 Modified Duke Criteria: Definition of terms used for the diagnosis of infective endocarditis (IE) (Modifications to original Duke criteria shown in boldface)

Major criteria
Blood culture positive for IE Typical microorganisms consistent with IE from 2 separate blood cultures: Viridans streptococci, *Streptococcus bovis,* HACEK group, *Staphylococcus aureus;* or Community-acquired enterococci, in the absence of a primary focus; or Microorganisms consistent with IE from persistently positive blood cultures, defined as follows: At least 2 positive cultures of blood samples drawn >12 h apart; or All of 3 or a majority of ≥4 separate cultures of blood (with first and last sample drawn at least 1 h apart) **Single positive blood culture for Coxiella burnetii or antiphase I IgG antibody titer > 1:800** Evidence of endocardial involvement Echocardiogram positive for IE **(TEE recommended in patients with prosthetic valves, rated at least "possible IE" by clinical criteria, or complicated IE [paravalvular abscess]; TTE as first test in other patients),** defined as follows: Oscillating intracardiac mass on valve or supporting structures, in the path of regurgitant jets, or on implanted material in the absence of an alternative explanation; or Abscess; or New partial dehiscence of prosthetic valve New valvular regurgitation (worsening or changing of pre-existing murmur not sufficient)
Minor criteria
Predisposition, predisposing heart condition or injection drug use Fever, temperature > 38 °C. Vascular phenomena, major arterial emboli, septic pulmonary infarcts, mycotic aneurysm, intracranial hemorrhage, conjunctival hemorrhages, and Janeway's lesions Immunologic phenomena: glomerulonephritis, Osler's nodes, Roth's spots, and rheumatoid factor Microbiological evidence: positive blood culture but does not meet a major criterion as noted above[a] or serological evidence of active infection with organism consistent with IE **Echocardiographic minor criteria eliminated**

Note: TEE, transesophageal echocardiography; TTE, transthoracic echocardiography
[a]Excludes single positive cultures for coagulase-negative staphylococci and organisms that do not cause endocarditis
From: Li JS, et al. [10]. Reproduced with permission, Oxford University Press

Table 19.2 Definition of Endocarditis from modified Duke criteria (Modifications to original Duke criteria shown in boldface)

Definite infective endocarditis
Pathologic criteria (1) Microorganisms demonstrated by culture or histologic examination of a vegetation, a vegetation that has embolized, or an intracardiac abscess specimen; or (2) Pathologic lesions; vegetation or intracardiac abscess confirmed by histologic examination showing active endocarditis Clinical criteria[a] (1) 2 major criteria; or (2) 1 major criterion and 3 minor criteria; or (3) 5 minor criteria
Possible infective endocarditis
(1) **1 major criterion and 1 minor criterion;** or (2) **3 minor criteria**
Rejected
(1) Firm alternate diagnosis explaining evidence of infective endocarditis; or (2) Resolution of infective endocarditis syndrome with antibiotic therapy for ≤4 days; or (3) No pathologic evidence of infective endocarditis at surgery or autopsy, with antibiotic therapy for ≤4 days; or (4) Does not meet criteria for possible infective endocarditis, as above

[a]See Table 19.1 for definitions of major and minor criteria
From: Li JS, et al. [10]. Reproduced with permission, Oxford University Press

indwelling lines in ill newborns and patients with chronic diseases, and (3) increased intravenous drug abuse.

Over the past 2 decades, CHD has become the predominant condition for IE in children greater 2 years of age in developed countries [3]. Before 1970, it was estimated that 30–50% of pediatric IE cases in the United States had underlying rheumatic heart disease [4]. However, it is unusual now to have IE from rheumatic heart disease in developed countries. Patients at greatest risk of IE are children with unrepaired or palliated CHD (ventricular septal defect, aortic valve abnormalities, patent ductus arteriosus, tetralogy of Fallot), those with implanted prosthetic material, and patients who have had a prior episode of IE [3, 5–7]. An increasing number of children with IE have had previous sur-

gery for CHD, and postoperative IE is a long-term risk after corrective surgery for complex cyanotic CHD when there is a residual defect or when surgical shunts or prosthetic materials have been left in place [1]. It can also occur in the absence of structural heart disease in neonates and pediatric patients with complex medical problems requiring indwelling central catheters, accounting for 8–10% of pediatric cases [8, 9]. In older patients, IE without CHD accounts for 25–45% of cases [8].

The diagnosis of IE is not always straightforward. To assist in the diagnosis, the modified Duke criteria are utilized; these criteria incorporate clinical, laboratory, pathologic, and echocardiographic evaluation (Table 19.1) [10]. The Duke criteria stratify patients into three main categories of definite IE, possible IE, and rejected IE based upon the presence of major and minor criteria (Table 19.2). Echocardiography—both transthoracic echocardiography (TTE) or TEE—is an important major criterion in the diagnosis of IE with special emphasis in the use of TEE in prosthetic valves or when the diagnosis is rated as possible IE by clinical criteria (Tables 19.1 and 19.2). Studies have demonstrated that when clinical evidence of IE is present, TEE improves the sensitivity of the Duke criteria to diagnose definite IE. The positive predictive value of the Duke criteria with TEE data for diagnosis of IE was 85% in patients with native valves and 89% in patients with prosthetic valves [11]. In adults, studies have demonstrated that the diagnostic sensitivity of TEE in IE is superior than TTE [12–19]. This is particularly true when IE is due to endocarditis of a prosthetic valve, an intracardiac abscess, and poor acoustic windows [17, 20]. In pediatric patients, the advantage of TEE over TTE is less apparent when TTE provides excellent imaging acoustic windows in infants and younger children. In general, TTE is considered adequate for the diagnosis of IE in young children, and TEE is reserved for those children with suboptimal imaging windows or inadequate TTE studies [21, 22].

Echocardiographic Manifestations of IE

The echocardiographic manifestations of IE include vegetations, valvular dysfunction, intracardiac abscesses, aneurysm formation, fistulous tracts, CHF, and/or pericardial effusions. Vegetations are the most characteristic findings of endocarditis. They are a mass of pathologic organisms nestled in platelets, red blood cells, and fibrin. Vegetations frequently are found in areas where the endothelium has been injured or disrupted by a high velocity jet or intravenous catheter. These can occur on valve surfaces but can also occur on cardiac chambers when the endothelial surface has been damaged (Figs. 19.1, 19.2, 19.3, 19.4, 19.5, Videos 19.1, 19.2, 19.3, 19.4, 19.5, 19.6). Vegetations can also occur on foreign materials such as prosthetic valve, conduit, shunts, or patches. The surface of the injured endothelium or prosthetic material serves as a nidus for platelet or fibrin deposition producing a thrombus at the site, initially sterile. With bacteremia, the circulating microorganisms can become adherent to meshwork resulting in an infected vegetation. More fibrin and platelet deposits occur, thus shielding the microorganism from host defense and allowing them to proliferate rapidly and produce further growth of the vegetation [1, 23, 24]. Vegetations can have a number of detrimental effects: (a) they can grow and destroy adjacent tissue; (b) organisms can be released continuously into the bloodstream, leading to persistent bacteremia and hematogenous seeding of remote sites; (c) pieces of the vegetation can break off and embolize to other organs (brain, lung, kidney), sometimes producing serious and even devastating complications; (d) antibody response to the infecting organisms leads to subsequent tissue injury by immune complex deposition [25]. By echocardiography, vegetations present as echogenic masses that are irregular in shape and variable in size, frequently located on the affected valve or nonvalvular structure or downstream to a high velocity jet (e.g. near a ventricular septal defect or valvar regurgitant jet). They are usually freely mobile,

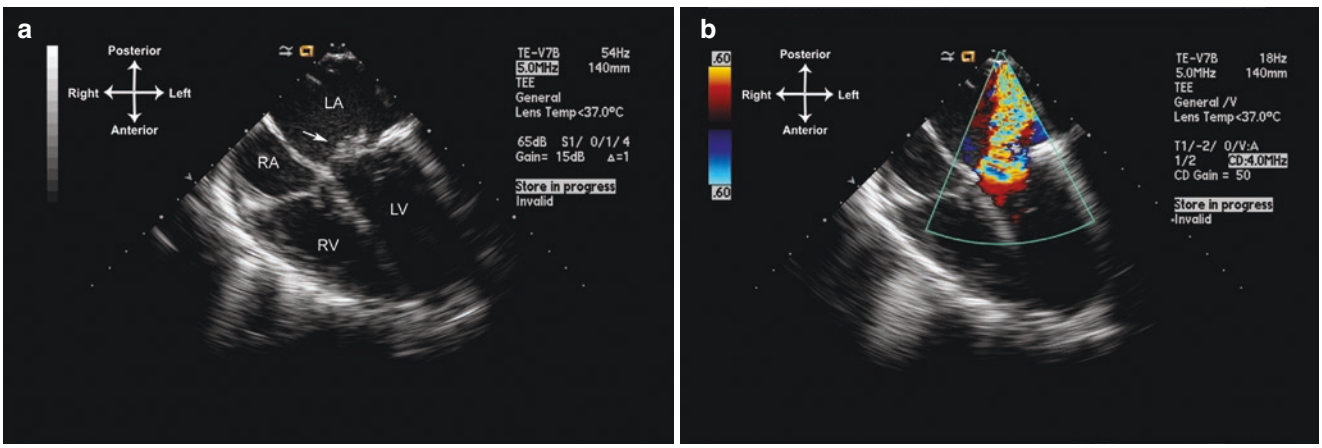

Fig. 19.1 Large vegetation (arrow) on the anterior leaflet of mitral valve (**a**), which resulted in chordal destruction and severe mitral regurgitation (**b**). Midesophageal four-chamber view (transducer angle 0°). *LA* left atrium, *LV* left ventricle, *RA* right atrium, *RV* right ventricle

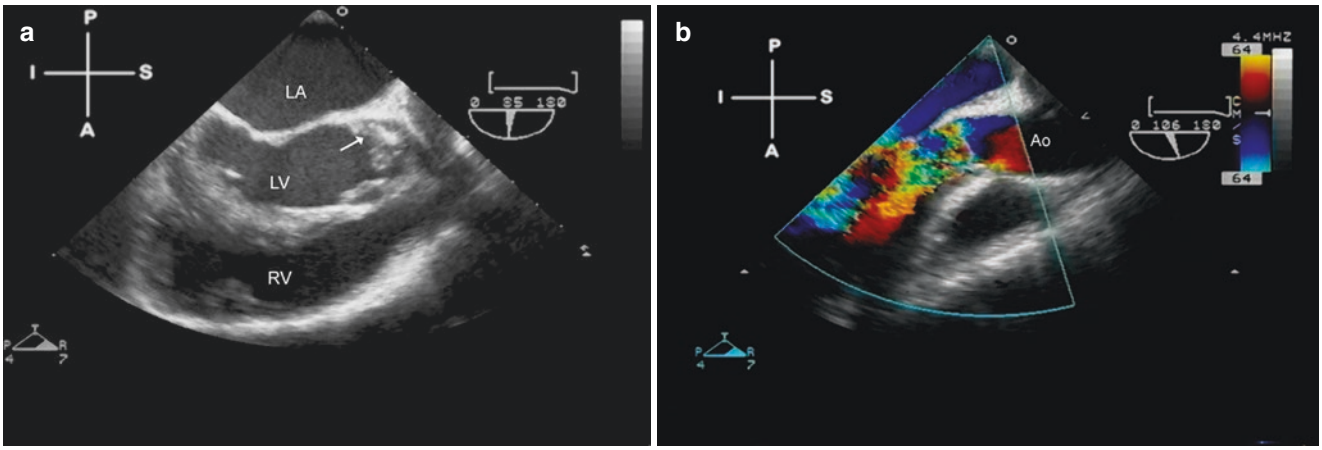

Fig. 19.2 Aortic valve endocarditis, seen from a midesophageal aortic valve long axis view (transducer angle 85°–106°). (**a**) Shows a prominent vegetation (arrow) on the left coronary cusp, which has caused significant cusp destruction and resulted in severe aortic valve regurgitation (**b**). *Ao* ascending aorta, *LA* left atrium, *LV* left ventricle, *RV* right ventricle

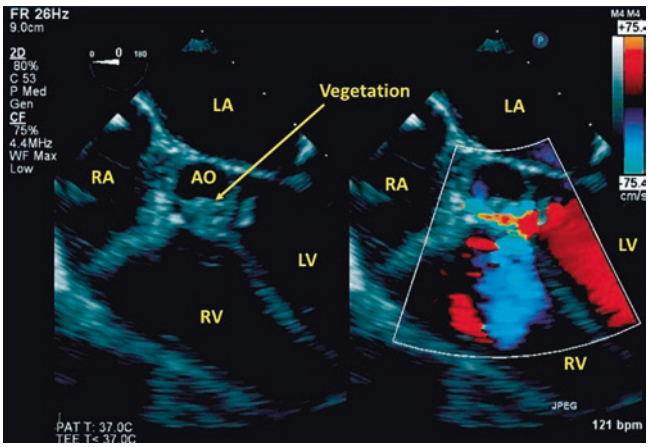

Fig. 19.3 A patient with *Staphylococcus aureus* bacteremia who had a transthoracic echocardiogram showing a large mass on the aortic valve with fibrinous strands. A vegetation is seen on the aortic valve from endocarditis in the midesophageal five-chamber view. There is a ventricular septal defect that occurred as a complication of the endocarditis, and color Doppler shows flow across the defect

oscillating with the cardiac cycle, and can move back and forth within the plane of the valve (Fig. 19.1, Video 19.1). Intracardiac vegetations are typically well seen by TEE.

Valvular dysfunction from IE may result from ruptured chordae with prolapsing or flail leaflets, fenestrations in the valve cusps, or torn leaflets. All of these lead to disruption of valvar function and resultant valvar regurgitation, often to a significant degree. It is not uncommon to see vegetations in association with valvar disruption, as evidence of the destructive process from IE. Significant valvular regurgitation can progress to CHF with a toxic appearance of the patient The amount of regurgitation can be evaluated by vena contracta width, and the regurgitant jet area or effective orifice obtained from color flow Doppler [26]. Examples of valve disruption and accompanying vegetation are shown in Figs. 19.1 and 19.2, Videos 19.1 and 19.2.

Intracardiac abscess forms when the infectious process extends to adjacent structures. Most commonly, this occurs with the aortic valve, when the infectious process extends into the weakest area of the annulus such as the membranous septum, potentially producing a ventricular septal defect (Fig. 19.3, Video 19.3). In some cases, the infectious process can involve the atrioventricular node, resulting in heart block. Perivalvar abscess formation can occur in 10–40% of all native IE, most commonly in the native aortic valve, and less commonly in the native tricuspid or mitral valve [27]. Perivalvar abscesses are seen in 56–100% of patients with prosthetic valve IE [27]. The echocardiographic appearance of abscess formation is an echo-free space with purulent fluid within the wall surrounding the affected valve or extending into the adjacent tissue. In patients with an abscess surrounding the prosthetic valve, there may be dehiscence of the valve. The preferred mode of evaluation of intracardiac abscess is TEE, which has been shown to yield a higher sensitivity than TTE for the diagnosis of abscesses associated with endocarditis [17]. An example of an abscess that formed around a prosthetic aortic valve is shown in Fig. 19.4, Video 19.4.

Aneurysm formation occurs when the infectious process extends to an adjacent vessel wall, causing thinning and destruction of the wall (Fig. 19.5, Video 19.5). This is seen in native aortic valve IE, when the sinus of Valsalva and adjacent cardiac structure form a fistulous tract creating a sinus of Valsalva aneurysm or a fistulous tract forms into the pericardial space [28, 29]. In this setting, TEE will demonstrate the aneurysmal dilation of the vessel wall, and color flow Doppler will demonstrate systolic/diastolic (or continuous) flow between the aorta and the receiving chamber (Fig. 19.5, Video 19.5). Pseudoaneurysm formation can also occur in

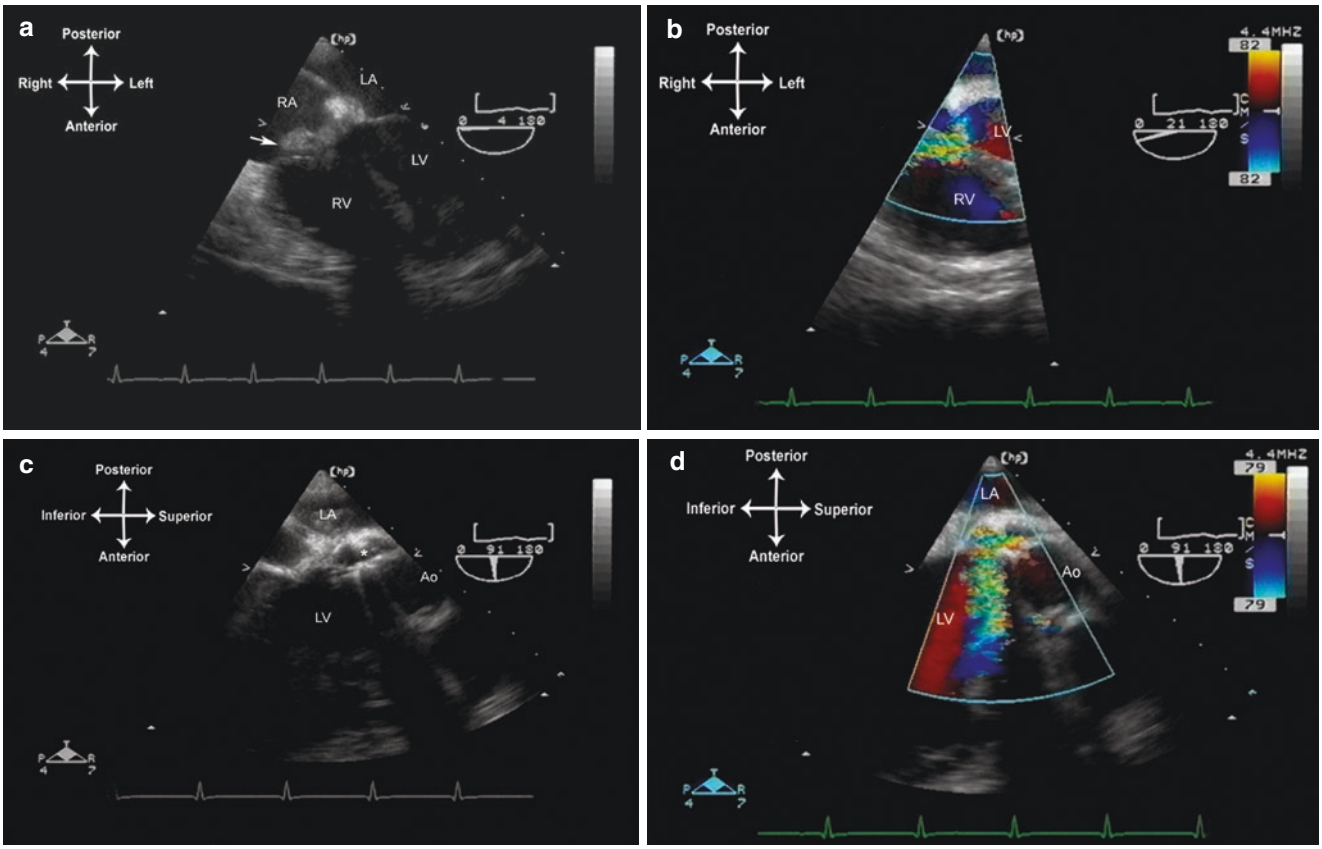

Fig. 19.4 Endocarditis in a patient with a prosthetic aortic valve (St. Jude). (**a**, **b**) The midesophageal four-chamber view demonstrates a perivalvar abscess that extends into the noncoronary cusp, causing a fistulous tract communicating with the right atrium. A large vegetation (arrow) has developed in this area and shunting is seen into the right atrium. (**c, d**) Modified midesophageal aortic valve long axis view, angle about 90°. There is marked aortic regurgitation seen through an area of valve dehiscence (*). *Ao* aorta, *LA* left atrium, *LV* left ventricle, *RA* right atrium, *RV* right ventricle

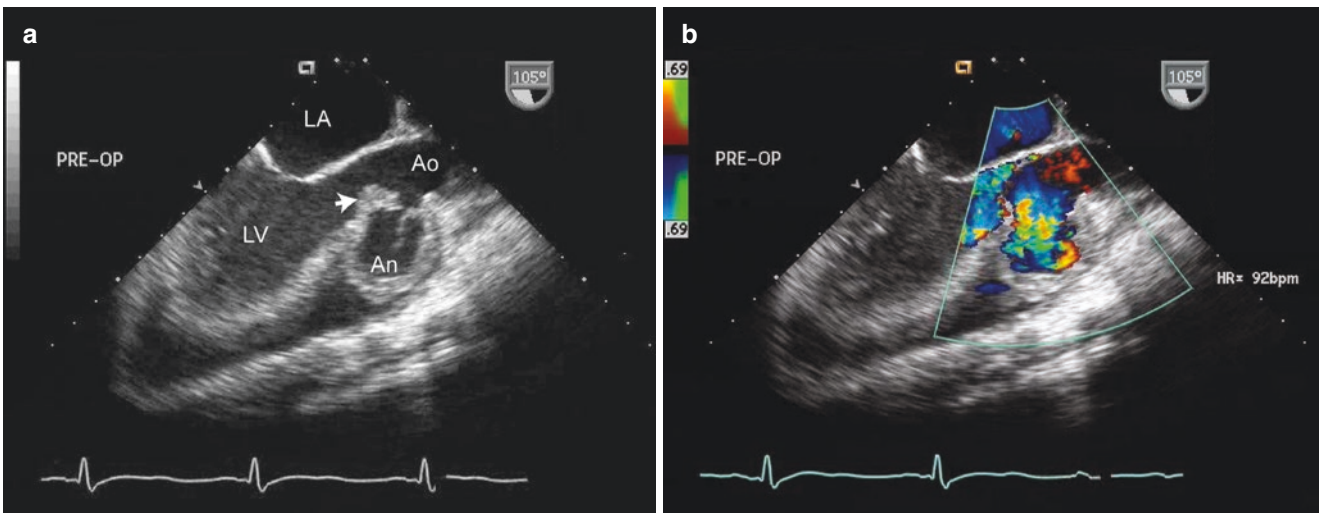

Fig. 19.5 Infected sinus of Valsalva aneurysm from aortic valve endocarditis, obtained from the midesophageal long axis view. (**a**) Shows a large vegetation of the aortic valve (arrow) and erosion of the right sinus of Valsalva, producing a large aneurysm (An). (**b**) Shows blood filling the aneurysm during diastole. *Ao* ascending aorta, *LA* left ventricle, *LV* left ventricle

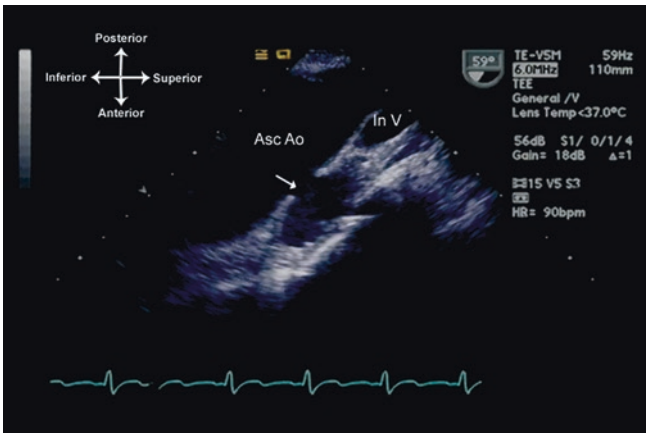

Fig. 19.6 Infected pseudoaneurysm off ascending aorta. This TEE was performed to evaluate the aortic valve in a patient with a previous aortic valve surgery and persistent fungemia. A large pseudoaneurysm (arrow) was discovered using the upper esophageal view, transducer angle 60°. In surgery, the pseudoaneurysm was found to be infected and filled with fungus. Note that the superior portion of aorta and innominate vein can be seen well in this patient by TEE. Asc Ao, ascending aorta; In V, innominate vein

foreign material such as suture material and biologic grafts [30, 31] (Fig. 19.6, Video 19.6).

Congestive heart failure is a complication of IE and is associated with poor prognosis [32, 33]. It can be a result of valvular and myocardial dysfunction, septic emboli to the coronaries resulting in myocardial ischemia, sudden intracardiac shunts from fistula formation, or abscess formation resulting in heart block. Acute CHF is more frequently seen in left sided infections in the aortic valve (29%) and the mitral valve (20%) than in the tricuspid valve (8%) [27]. A pericardial effusion can also be seen in patients with IE; it can be infectious, resulting from hematogenous seeding of the pericardium, or as a direct extension from intracardiac IE (e.g. perforation of a perivalvar abscess). Rarely, it can be occur as a reactive/serous effusion [34].

Goals of TEE Imaging in IE

The evaluation of IE by TEE can occur in several settings. It can be performed in the ICU or ambulatory setting, serving as either diagnostic evaluation for suspected IE or as a monitoring procedure for a patient receiving treatment for known IE. It also plays a vital role in the intraoperative setting. Preoperatively, TEE is used to assess not only the vegetation or abscess, but also valvar function and the surrounding cardiac structures. When applicable, prosthetic valve dehiscence and pseudoaneurysm formation can also be evaluated. Postoperatively, TEE is used to assess the results of operative repair or valve replacement, and guide perioperative hemodynamic management [34, 35].

The goals of TEE imaging in IE are to evaluate for vegetations, valvular dysfunction, intracardiac abscesses, aneurysm formation, fistulous tracts, abnormalities supporting congestive physiology, and/or pericardial effusions. A complete study with upper esophageal, midesophageal, transgastric, and deep transgastric views (Chap. 4) should be used to evaluate for manifestations of IE. If vegetations are found, the appearance and motion should be evaluated in multiple planes, and measurements made. The risk of emboli appears to be greatest when the vegetation is >10 mm on the anterior leaflet of the mitral valve [27]. Attention must be paid to valve leaflet anatomy and motion both by two-dimensional (2D) imaging and color flow Doppler. Valve perforation and chordal disruption must be inspected, and three-dimensional (3D) TEE imaging can be helpful in delineating the perforated site and chordal disruption with flail leaflets. In cases of aortic valve endocarditis, abscess and aneurysmal formation must be inspected. If IE occurs in prosthetic valves, then a thorough examination of the valve leaflet motion is mandatory, as well as inspection for any possible paravalvular leak around the sewing ring that might suggest perivalvar abscesses and dehiscence. Myocardial function and the presence of pericardial effusion should also be evaluated.

Three caveats are important to consider. First, even with TEE, not all vegetations will be visible, particularly if the vegetations are smaller than the resolution limits of the TEE probe and/or TEE imaging is suboptimal. This is an important consideration in patients with operated and unoperated CHD, who can have vegetations located in areas not readily visible by TEE (e.g. a Blalock-Taussig shunt). Studies have shown that—irrespective of whether TTE or TEE is used—patients with CHD and IE are less likely to have visible vegetations [36]. Thus, the echocardiographic data should be considered in the context of the entire clinical picture, as noted with the Duke criteria listed above. In some cases, if IE is still suspected, a TTE or TEE can be performed 7–10 days later to determine if a vegetation or abscess has appeared [27, 36, 37]. The second important caveat is that not all echogenic masses represent vegetations. Sterile thrombi, tumors, irregular valve excrescences, and foreign material (such as suture material) can sometimes resemble vegetations. Again, the echocardiogram should be reviewed in conjunction with the entire clinical picture. Also, if previous echocardiograms are available (either transthoracic or transesophageal), these can be very useful to make direct comparisons to determine whether the abnormal finding is new or longstanding. New findings are much more suspicious for IE. The last important caveat is that not all vegetations are infectious. A number of medical conditions can produce sterile vegetations adherent to valvar surfaces. Examples of such conditions include systemic lupus erythematosus (Libman-Sacks endocarditis), and nonbacterial thrombotic endocarditis (NBTE, also known as marantic endocarditis). The latter can occur as complication of malignancy, uremia, burns, hypercoagulable states, or autoimmune diseases, and it has been found in approximately 1.2% of all autopsy patients, although the reported incidence is between

0.3–9.3% [25, 38]. In fact, Libman-Sacks endocarditis is felt to be a form of NBTE [39]. These vegetations are usually seen on the valve closure contact line of the atrial surface of the atrioventricular (AV) valves, and the ventricular surface of the semilunar valves. In many cases, the vegetations are benign and clinically unapparent. However, systemic embolization has been described in up to 30–50% of patients [38–40], with a tendency towards embolization to the brain, kidney, spleen, mesenteric bed, or extremities [39, 41].

Cardiac Thrombi

Cardiac thrombi can occur in the setting of poor cardiac function and stasis of blood, especially in cases of dilated cardiomyopathy. The use of TEE is complementary to TTE assessment for thrombi in the pediatric population. Generally, cardiac thrombi can be seen by TTE except for those instances of poor acoustic windows (such as in intensive care patients). Thrombi can vary in echogenic appearance and location. They are echogenic, homogeneous in density, irregular in shape (they can be broad or pedunculated), and in some instances can have calcifications within the thrombus. They may attach to the endocardial surface or atrioventricular valve, or to foreign material. In patients with atrial arrhythmias such as atrial fibrillation, they can be located within the atrial appendages. In the critical care setting, they are commonly found at the end of an indwelling catheter near the innominate vein, superior vena cava (SVC), or right atrium. TEE can be used to evaluate the size, attachment point, and the extent of an SVC or right atrial thrombus. In the mid to upper esophageal views, the probe can be rotated rightward with angle to 90°, allowing for visualization of the sagittal plane of the SVC return to the right atrium. A catheter can be seen in this view, and if there is a thrombus, it can be visualized and the size should be measured (Fig. 19.7, Video 19.7). If there is obstruction to the SVC, then a deep transgastric view can be used with rightward turning and anteflexion of the probe, to achieve posterior angulation and visualize the SVC flow as it enters the right atrium. The mean gradient can be measured using spectral Doppler interrogation.

Though less common in children, patients with atrial fibrillation or severe mitral stenosis can have thrombi in the left and right atrial appendages [42–44]. In adult studies, the incidence of left atrial thrombus in patients with atrial fibrillation is between 10–15% and that of a right atrial thrombus of 0.4–7.5% [45]. These thrombi are often difficult to identify by TTE and can be difficult to distinguish from pectinate muscles [46]. The use of TEE provides excellent visualization of the left and right atrial appendages [47, 48]. The right atrial appendage can be examined in the midesophageal bicaval view, transducer angle 90°–110°, and it is seen anterior to the SVC/right atrial junction. The transducer angle can then be rotated to 0° to visualize the right atrial appendage from a different plane. The left atrial appendage can be viewed in the midesophageal left atrial appendage (ME LAA) view with leftward probe rotation and a transducer angle of 90° (although the transducer angle can be varied from 0° to 90° for optimal visualization of the thrombus) (Fig. 19.8, Video 19.8). Live 3D imaging can also be used, rotating the image so that the left atrial appendage can be seen in different views. It is important to inspect both the right and left atrial appendages to distinguish thrombi from pectinate muscles, crista terminalis, Chiari network, and Eustachian valves—all of which are normal anatomic components found in the atria and atrial appendages [47, 49–51].

Fig. 19.7 Thrombus (arrow) in the superior vena cava, probably associated with a catheter. Seen from a modified midesophageal bicaval view, (transducer angle 118°). *LA* left atrium, *RA* right atrium

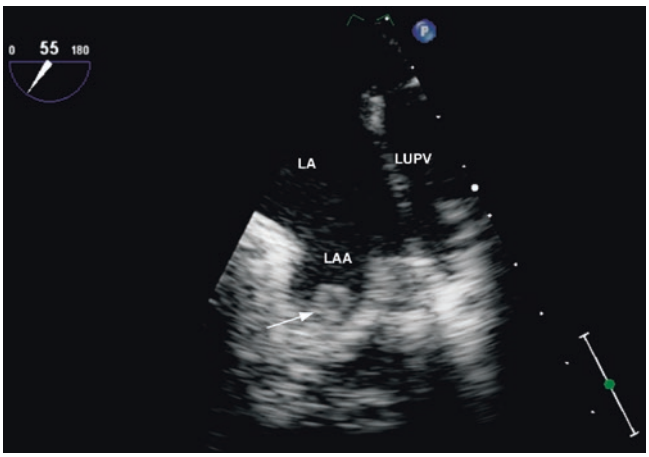

Fig. 19.8 Modified midesophageal left atrial appendage view (transducer angle 55°) showing a thrombus (arrow) in the left atrial appendage (LAA) in a patient with atrial fibrillation. *LA* left atrium, *LUPV* left upper pulmonary vein

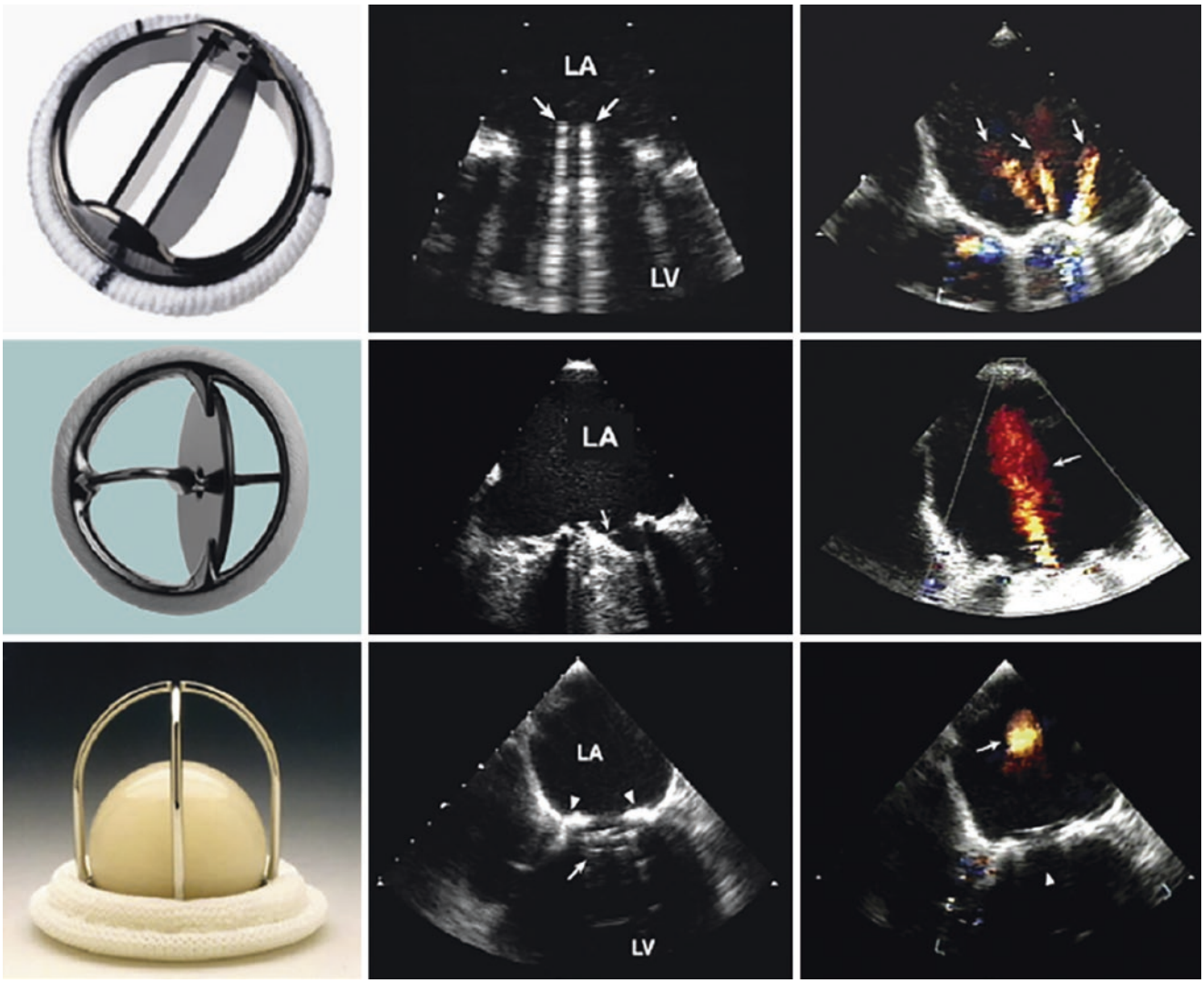

Fig. 19.9 Examples of bileaflet (St Jude, **a**), single-leaflet (Medtronic-Hall, **b**), and caged-ball (Starr-Edwards, **c**) mechanical valves and their transesophageal echocardiographic characteristics taken in the mitral position in diastole (middle) and in systole (right). The arrows in diastole point to the occluder mechanism of the valve and in systole to the characteristic physiologic regurgitation observed with each valve. Reprinted from Zoghbi et al. [52]; with permission from Elsevier

Prosthetic Valves

There are two types of prosthetic valves, mechanical and biologic, that are used for surgery (both mechanical and biologic); biologic valves are used for transcatheter valve replacement. Mechanical heart valves contain nonbiologic materials (polymers, metal, carbon) in all parts of the prosthesis: the valve ring, sewing cuff, and orifice occluder. A number of mechanical valves have been developed over the past 50 years, essentially of three major types. The first type to be developed was the caged ball valve, consisting of a silastic ball with a circular sewing ring and a cage formed by 3 metal arches. The most notable of these was the Starr-Edwards valve (Fig. 19.9c), though similar valves have been produced including the Smeloff-Cutter valve. While these valves are no longer implanted, many patients who received these valves are still alive, and continue to be followed regularly. The second type of mechanical valve is the monoleaflet valve, in which a single disk is secured by lateral or central metal struts, and surrounded by a sewing ring. The disk, generally made of extremely hard carbon (pyrolytic carbon), opens by tilting at an angle (about 60°–80°), resulting in 2 orifices of different sizes. Typical examples of this include the Bjork-Shiley (discontinued), and the Medtronic-Hall valve (Fig. 19.9b). The third major type of mechanical valve is the bileaflet tilting disk valve, made of two semicircular pyrolytic carbon disks attached by hinges to a rigid valve sewing ring. In the open position the valve leaflets tilt to an opening angle of 75°–90°, resulting in three orifices: a small slit-like orifice centrally between the two leaflets, and two semicircular orifices laterally. Of the three types of mechanical valves, this type provides the most natural blood flow, greater effective orifice area for a given valve size,

and is also the least thrombogenic. Currently, the most commonly implanted mechanical valves are the bileaflet valves, notably the St. Jude Medical (Fig. 19.9a) and Carbomedics bileaflet tilting disk valves. They are available in a variety of sizes (from 15–33 mm) suitable for both pediatric and adult patients. The mechanical valves have a proven record of durability, though they require ongoing anticoagulation therapy, and there are ever-present risks of thrombosis and endocarditis of the valve. In many types of mechanical valves, separate aortic and mitral versions are available. However, for a number of the mechanical valves, implantation has been performed in any of the four valve positions.

Biologic heart valves are derived from human or animal tissue, and certain valves contain nonbiologic material as well, such as metal and fabric. Human tissue valves fall into two categories: *homografts* (*allografts*) and *autografts*. Homograft valves are cryopreserved cadaveric aortic and pulmonary valves, generally used as pulmonary or aortic valve replacements (Fig. 19.10). They come in a variety of sizes, depending upon donor availability. In contrast, an autograft represents the patient's own valve translocated from one site to another. Usually, the autograft is the pulmonary valve translocated to the aortic position (Ross procedure) or rarely the mitral position (Ross II), with a homograft valve being placed in the original pulmonary position [53–55]. Biologic valves derived from animal tissue are known as *xenograft* (or *heterograft*) valves; the most commonly used animal tissues are porcine aortic valve and bovine pericardium, and the tissues are fixed with glutaraldehyde. These valves come in two major forms. *Stented* biologic valves contain a sewing ring and struts composed of nonbiologic material (metal, cloth), and valve tissue is sewn onto the fabric covering the struts.

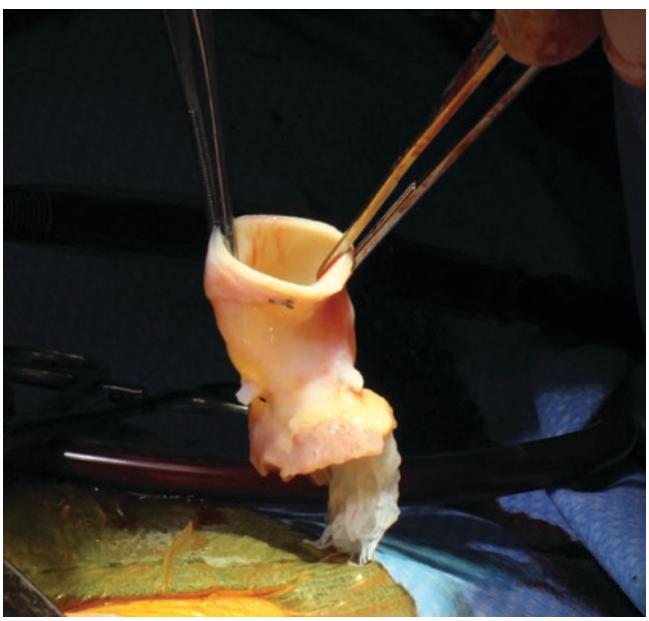

Fig. 19.10 Aortic homograft, following thawing and prior to implantation as a right ventricle to pulmonary artery conduit

Both porcine valve (Fig. 19.11a) and bovine pericardium are used with these types of valves. *Stentless* biologic valves contain no struts or sewing ring, which leaves more room for blood flow. Stentless xenograft valves derive primarily from harvested porcine aortic valves (Fig. 19.11b). Of note, human homograft and autograft valves fall into the category of unstented biologic valves, since they contain no sewing ring or struts. This is because the entire homograft/allograft root (containing the valves) is harvested, thus the intrinsic structural support for the valve leaflets remains intact. Another category of bioprosthesis that has gained popularity is the Contegra pulmonary valve conduit. The Contegra conduit is a bovine jugular vein preserved in glutaraldehyde, and it contains a valve with three leaflets; the leaflets are similar to a human semilunar valve (Fig. 19.12). Since it is derived from a venous vascular structure, it is felt to be best suited for conditions of lower pressure such as the pulmonary circuit, and therefore it is used primarily for congenital heart surgeries in which a right ventricle to pulmonary artery conduit is needed such as the Ross procedure, tetralogy of Fallot, truncus arteriosus, etc. [56]. Thus it serves as an alternative to the homograft, and has achieved comparable short to intermediate term results [57–59]. Strictly speaking, it is a valved conduit (not solely a biologic valve), but it is used in a number of operations in which a valve is necessary. As will be discussed below, the bovine jugular valve is also used for transcatheter valve technology.

Over the years, a large number of different valve prostheses (both mechanical and biologic) have been developed, in a variety of valve sizes and profiles. Development continues at a rapid pace, with novel alternatives currently in development or advanced clinical trials. A list of some of the better-known biologic and mechanical valves is given in Table 19.3; this list is by no means exhaustive, and new models and types are periodically being introduced. A full discussion and elaboration of the many individual valves would require a separate chapter. For further discussion, the reader is referred to a number of references providing more detailed coverage of the topic [60–64].

Both mechanical and biologic valves can be used to replace a stenotic or regurgitant valve in any of the four valve positions. The preference for valve replacement type varies depending upon the desired site of implantation, and includes considerations such as age of the patient, evidence-based effectiveness of valve prosthesis alternatives for the intended valvar position, valve durability, valve size availability, and the need for ongoing medical therapy. Mechanical prostheses boast greater durability, but this must be balanced with the need for constant anticoagulation and the ever-present risks of bleeding, thrombosis and endocarditis. Conversely, biologic valves do not generally require significant anticoagulation, but their durability can be much more variable. While there are multiple options for each valve site, some generalizations can be made [65]. For pulmonary valve

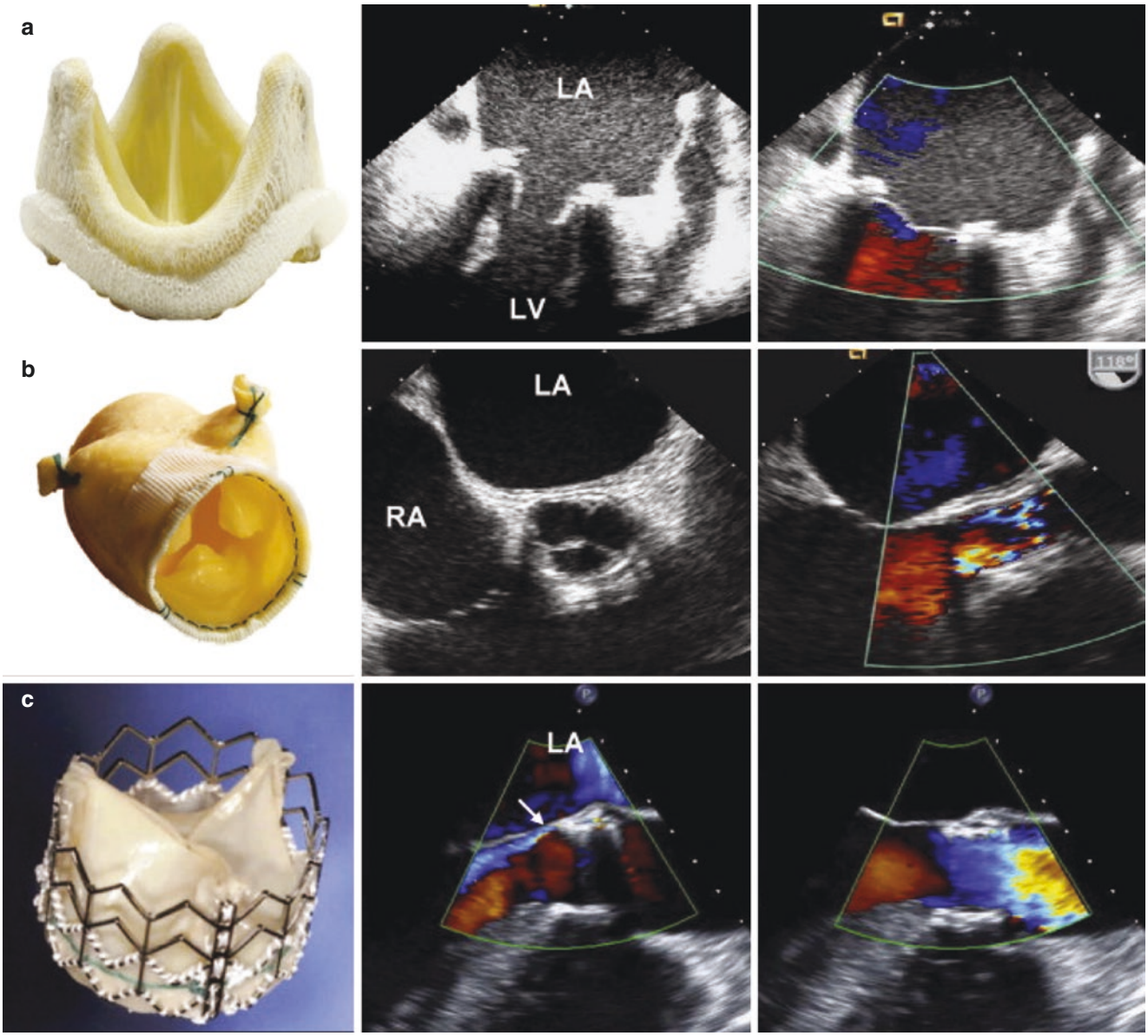

Fig. 19.11 Examples of stented (**a**), stentless (**b**), and percutaneous biologic valves (Edwards SAPIEN, **c**) and their echocardiographic features in diastole (middle) and in systole (right) as seen by TEE. The stentless valve is inserted by the root inclusion technique. Mild paravalvular aortic regurgitation in the percutaneous valve is shown by arrow. Reprinted from Zoghbi et al. [52]; with permission from Elsevier

replacement, biologic valves—notably homograft (allograft) and heterograft (porcine, bovine pericardial)—are generally preferred, though some investigators have advocated for mechanical valves [66]. For tricuspid, either a mechanical valve or stented porcine valve is generally used. For the aortic valve, both biologic (homograft, heterograft, pulmonary autograft) and mechanical prosthetic valves are utilized. A number of stented and unstented bioprosthetic xenograft valves have been developed for the aortic valve position. For the mitral valve, mechanical prostheses predominate in children and adults, although stented biologic valves (porcine and bovine pericardial) are selectively used in the adult group due to other important considerations (such as pregnancy and the risk of warfarin embryopathy) [65].

One of the most important and exciting new areas in prosthetic valve technology has been the development of catheter-based, implantable prosthetic valves, also known as transcatheter heart valves or THVs. Valve leaflets composed of biologic tissue are mounted in an expandable metal frame, which can then be delivered using various transcatheter techniques and precisely placed in the location of the diseased or absent valve. Several of these THVs are well-known, having already gained a large clinical experience. The **Melody valve** is a bovine jugular valve mounted on a platinum iridium stent, and delivered by a 22 F balloon in balloon catheter delivery system [67]. It is primarily designed for pulmonary valve replacement, and in the United States it is currently used only in an existing right ventricular outflow conduit,

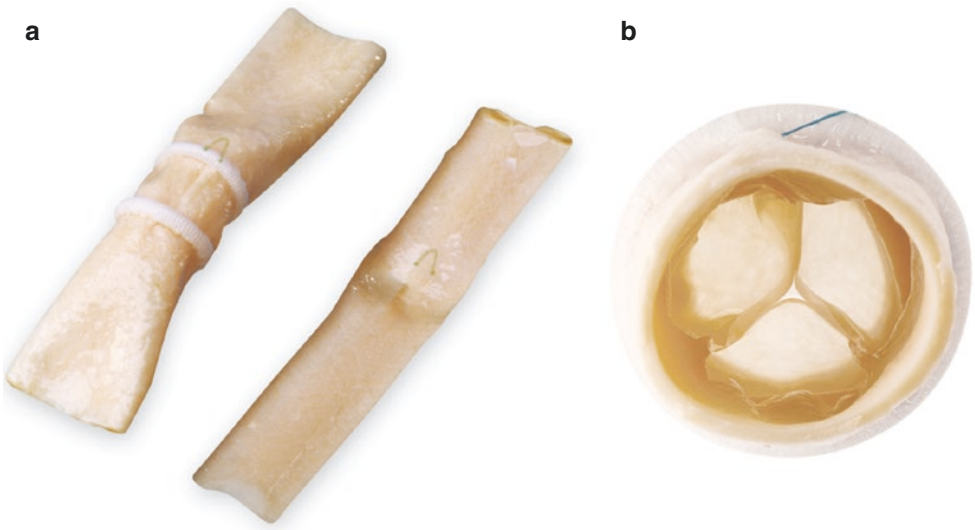

Fig. 19.12 Contegra bovine jugular vein, containing a trileaflet valve that is similar to a human semilunar valve

Table 19.3 Typical biologic and mechanical valves

Valve name/type	Manufacturer	Valve type/origin
Biologic—Human		
Autograft		Pulmonary autograft
Allograft (Homograft)	Cryolife	Harvested cadaveric aortic, pulmonary homograft
Monocusp, bicuspid		Surgically handsewn valve using autologous pericardium
Biologic—Heterograft		
Stented		
Hancock II	Medtronic	Porcine
Mosaic	Medtronic	Porcine
Carpentier-Edwards	Edwards-Lifesciences	Porcine
Epic	St Jude	Porcine
Biocor	St Jude	Porcine
Trifecta	St Jude	Bovine pericardial
Carpentier-Edwards Perimount Magna	Edwards Lifesciences	Bovine pericardial
Mitroflow	Sorin Biomedica	Bovine pericardial
Soprano	Sorin Biomedica	Bovine pericardial
Inspiris	Edwards Lifesciences	Bovine pericardial
Stentless		
Freestyle	Medtronic	Porcine
Toronto SPV	St Jude	Porcine
Prima Plus	Edwards Lifesciences	Porcine
Pericarbon Freedom	Sorin Biomedica	Bovine pericardial
3F Therapeutics Stentless Equine	3F Therapeutics	Equine pericardial
Mechanical		
Starr-Edwards	Edwards Lifesciences	Ball-in-cage
Bjork-Shiley	Pfizer	Single leaflet tilting disk
Medtronic-Hall	Medtronic	Single leaflet tilting disk
St Jude Medical	St Jude	Bileaflet tilting disk
CarboMedics	Sorin-CarboMedics	Bileaflet tilting disk
ATS Medical	ATS Medical	Bileaflet tilting disk
On-X	On-X Life Technologies	Bileaflet tilting disk
Percutaneous—Biologic		
Melody	Medtronic	Bovine jugular valve mounted on platinum-iridium stent
SAPIEN	Edwards Lifesciences	Bovine pericardium leaflets mounted on stainless steel or cobalt chromium alloy (SAPIEN XT)
Evolut R (CoreValve)	Medtronic	Porcine pericardium leaflets mounted on self-expanding nitinol frame
Lotus	Boston Scientific	Bovine pericardial, self-expanding nitinol stent
Other		
SynerGraft	Cryolife	Tissue engineered decellularized allograft heart valve
Contegra	Medtronic	Valved conduit of bovine jugular vein

Used for transcatheter valve-in-valve implantation for failed surgical bioprosthetic valves

though in Europe it has also been used in patients with tetralogy of Fallot and a right ventricular outflow tract patch (using pre-stenting techniques) [68]. It has also been used in other positions such as failed AV valve bioprostheses (also known as "valve-in-valve" replacement) [67, 69, 70], native aortic valve replacement [69], and in the branch pulmonary arteries [71]. For transcatheter aortic valve replacement/implantation (also known as TAVR, or TAVI), there are two major devices currently available. The **Edwards SAPIEN** valve contains bovine pericardial leaflets sewn inside a stainless steel or cobalt chromium alloy frame. The inflow of the frame is covered with fabric to provide an annulus seal (Fig. 19.11c). The valve is positioned through a sheath (22–24F for the SAPIEN, 16–19F for the SAPIEN XT) either from the femoral artery, ascending aorta, or through the left ventricular apex (the latter two methods utilizing a hybrid surgical approach). Once positioned, the frame and valve are balloon expanded within the diseased native aortic valve, displacing the native leaflets. Rapid ventricular pacing is performed during implantation to reduce cardiac contraction during valve implantation [72]. This valve is also used for valve-in-valve replacement (mitral, tricuspid), and is undergoing trials for use in transcatheter pulmonary valve replacement (similar to the Melody valve) [67, 73]. See Chap. 13 for an example of TAVR using a SAPIEN valve. The other major valve for TAVR/TAVI is the **Medtronic Evolut R** and **Evolut Pro** systems. These valves are composed of porcine pericardial leaflets mounted in a self-expanding nitinol frame. They are delivered within a 14 or 16 F sheath, introduced percutaneously via femoral or subclavian artery access. Rarely, direct aortic access is utilized for delivery of the device. Once the sheathed device is located in the desired position, the device expands (and becomes deployed) by retraction of the sheath. Deployment does not require rapid ventricular pacing. To date, it has limited utility for valve-in-valve therapy.

It should be noted that research and development in THVs continues at a very rapid pace, and for all the different cardiac valves; in the near future one can expect to see a number of new valves in various stages of clinical trials [74, 75].

Echocardiographic Evaluation of Prosthetic Valves

Echocardiography is important in the evaluation of these valves before and after surgery, or during transcatheter interventions [52, 76]. Postoperative evaluation of the prosthetic valve includes assessment of function of the valve and anatomic appearance of the newly implanted valve. A comprehensive TEE assessment of prosthetic valve includes careful 2D imaging with color and spectral Doppler evaluation of flow across the valve. The prosthetic valve should be examined from multiple views, with emphasis on leaflet motion, appearance of the sewing ring, and presence of any abnormal echo density that might be attached to the prothesis. The valve must be well-seated, without excessive movement, otherwise dehiscence must be suspected [52]. Then the valve should be interrogated with color and spectral Doppler for possible paravalvular leaks, stenosis, or abnormal flow. However, it is important to remember that the intraoperative setting provides unique challenges for valvar assessment due to physiologic alterations from changing preload/afterload, inotropic support, open sternum, positive pressure ventilation, and general anesthesia (also discussed in Chap. 18—Intraoperative and Postoperative Evaluation).

The examination of the mechanical valve is different from a native valve, as increased spectral Doppler velocities are expected, and these will vary depending on the type of mechanical valve one is interrogating [52, 77, 78]. The mechanical bileaflet tilting disk valve (St. Jude valve) has one central orifice with two side orifices to allow for forward flow when it is open [52, 77] (Fig. 19.13a; Video 19.9). When it is closed, there are two small regurgitant ("washing") jets at the pivot points of the valve, angled centrally

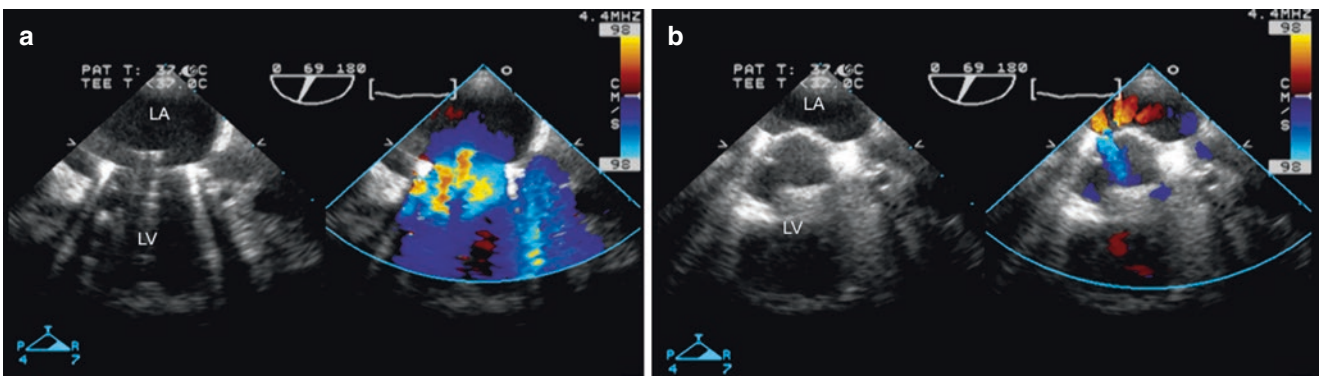

Fig. 19.13 Prosthetic mitral valve (bileaflet tilting disk), midesophageal mitral commissural view, transducer angle 69°. The transducer angle is rotated until both leaflets are profiled and open symmetrically in diastole (**a**) and systole (**b**). There is the usual color flow Doppler profile across the valve. *LA* left ventricle, *LV* left ventricle

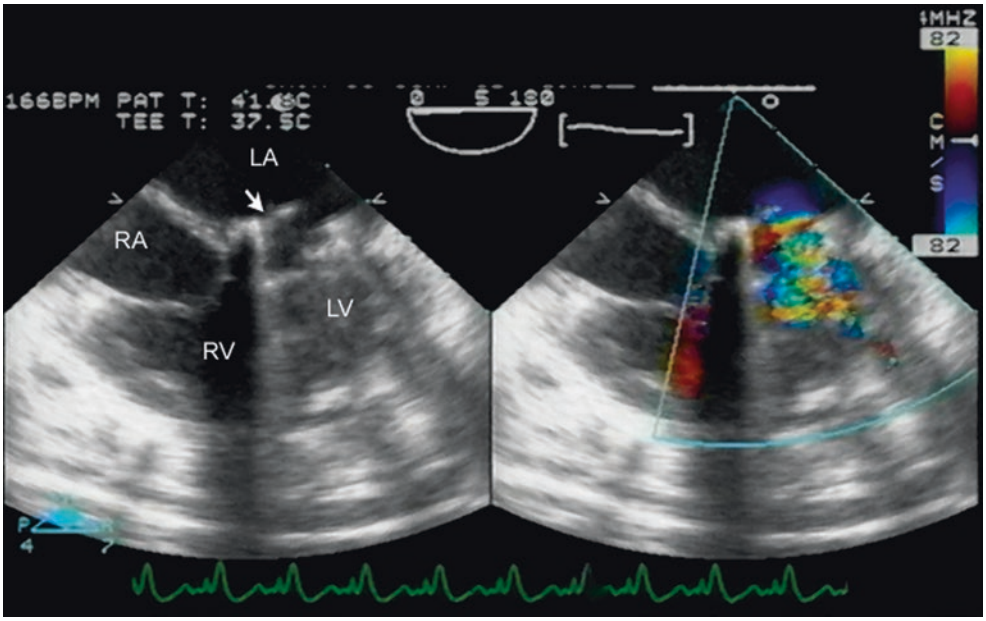

Fig. 19.14 Prosthetic mitral valve with a frozen leaflet (arrow), causing stenosis. Midesophageal four-chamber view, transducer angle 0°. *LA* left atrium, *LV* left ventricle, *RA* right atrium, *RV* right ventricle

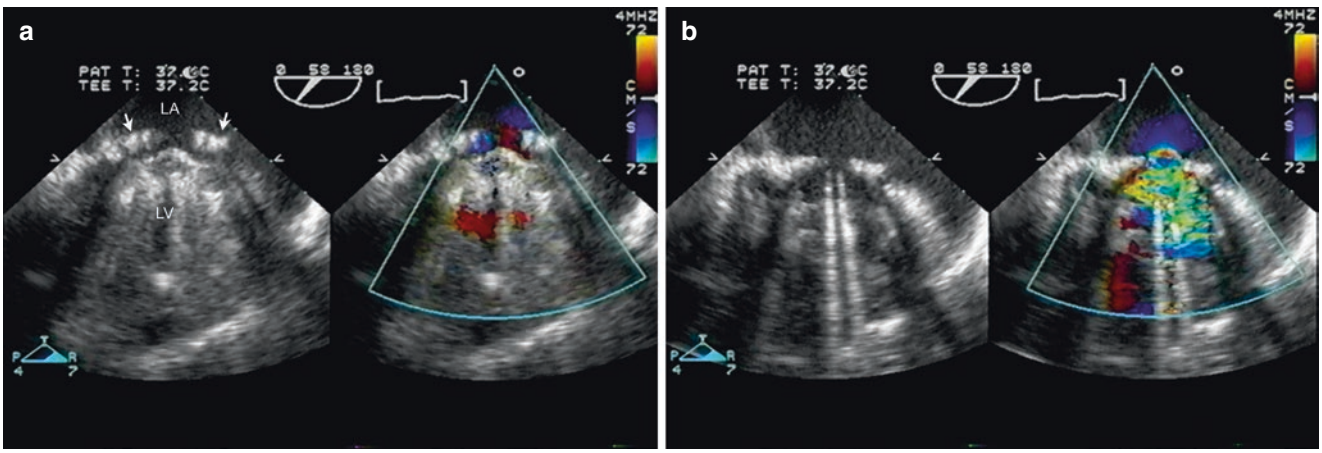

Fig. 19.15 Concentric pannus formation (arrows) above the mitral valve prosthesis (**a**), causing significant supravalvar narrowing, seen during diastole (**b**). Midesophageal view, transducer angle 58°. *LA* left ventricle, *LV* left ventricle

(Figs. 19.9, 19.13b) [79]. These small regurgitant jets are intended to prevent thrombus formation [79]. Abnormalities of the valve leaflet motion, vegetations, pannus formation, thrombus, paravalvular leaks, and paravalvular dehiscence can be seen well by TEE (Figs. 19.14, 19.15, 19.16, Videos 19.10, 19.11, 19.12) [79, 80]. Evaluating a mechanical aortic valve starts from the midesophageal plane, using a transducer angle between 0–120°. At 30°–40°, the long axis view of the valve can be evaluated with examination of the asymmetry of the valve leaflet position/motion and search for any paravalvular leaks. There can be acoustic shadowing from the midesophageal views, and this could necessitate evaluation from other windows. From the transgastric and deep transgastric views, the subaortic region can be evaluated and the valve motion can be visualized to assess for valvar regurgitation from color flow and spectral Doppler (Fig. 19.17, Video 19.13) [79]. These views avoid the shadowing artifacts that occurs in the midesophageal views. When evaluating atrioventricular mechanical valves, the midesophageal views from 0°–90° provide excellent visualization of the prothesis leaflets and leaflet motion from an edge-on view. Restricted leaflet motion and pannus formation can be well seen from these views. Chordal tissue and papillary muscles that are left in place after mechanical valve placement should not be confused with thrombus formation.

Evaluation of biologic prosthetic valves (stented or stentless) have less acoustic shadowing compared to the mechanical valves (Fig. 19.11). The stented valves have struts that are easily seen by echocardiography and the valve leaflets are thin. Stentless valves such as homografts, xenografts, and autografts are similar to native valves when imaged by TEE. Biologic prosthetic valves can be evaluated by 2D/3D imaging, color and spectral Doppler similar to native valves [81]. In the operating room, TEE is frequently used during

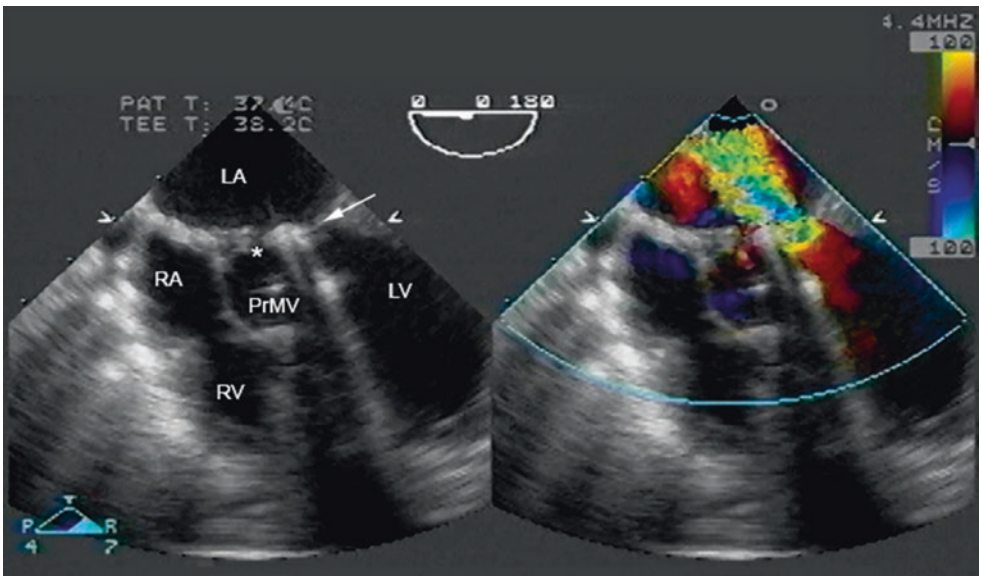

Fig. 19.16 Paravalvar regurgitation in a child who underwent mitral valve replacement with a mechanical bileaflet prosthesis (previous history of atrioventricular septal defect repair). Image obtained from a midesophageal four-chamber view (transducer angle 0°). The prosthesis was too large for the annulus and required insertion at an angle, which resulted both in a large area of paravalvular regurgitation (arrow) as well as a very small effective orifice (asterisk). *LA* left atrium, *LV* left ventricle, *PrMV* prosthetic mitral valve, *RA* right atrium, *RV* right ventricle

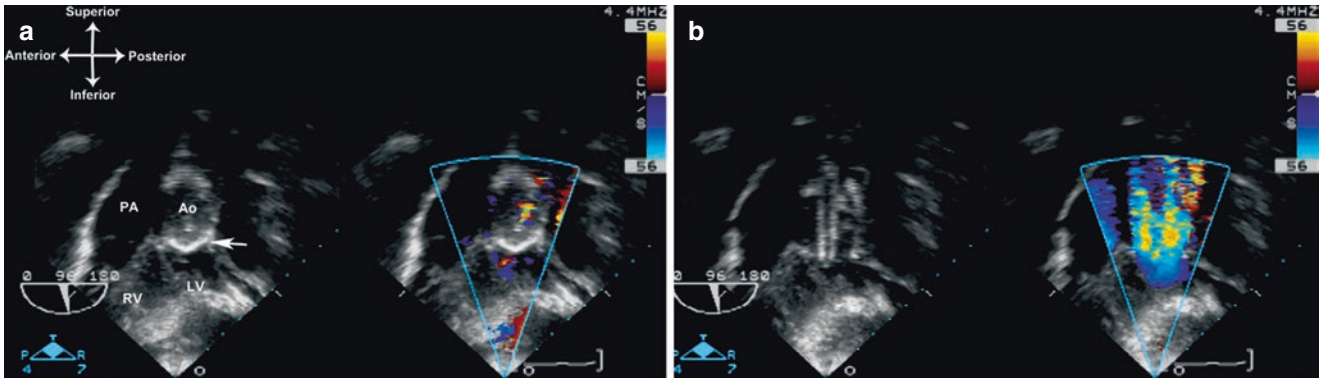

Fig. 19.17 Prosthetic aortic valve (bileaflet tilting disk) viewed from deep transgastric position, transducer angle 96°. The transducer angle has been rotated until both leaflets are profiled and symmetric leaflet motion is noted in diastole (**a**) and systole (**b**). The prosthetic valve position is marked by the arrow. This transducer position affords a good view of leaflet motion and flow across the valve, and also provides an excellent angle for spectral Doppler evaluation. *Ao* ascending aorta, *LV* left ventricle, *PA* pulmonary artery, *RV* right ventricle

surgery for valve replacement. In the critical care setting, if the patient is hemodynamically unstable with poor acoustic windows, then TEE is used to evaluate stenosis or regurgitation. The flow velocities through these valves immediately after the operation are used for comparison with later studies. Biologic prosthetic valves can become stenotic from calcification, thrombus formation or vegetation from infective endocarditis (Fig. 19.18, Videos 19.14, 19.15, 19.16).

Doppler Evaluation of Prosthetic Valves

For Doppler evaluation of prosthetic valves, the principles and techniques of valve interrogation and recording of flow velocity are similar to those used for evaluating native valve stenosis or regurgitation (see Chap. 9—Mitral and tricuspid valve evaluation and Chap. 13—Outflow tract anomalies) [82, 83]. However, a few general comments are worth noting. Prosthetic valve regurgitation is primarily assessed with Doppler evaluation, mainly using color flow techniques, though spectral Doppler evaluation is helpful as well. It is important to differentiate between "normal" and pathologic prosthetic valve regurgitation. A mild degree of regurgitation is normally seen in virtually all mechanical valves (Fig. 19.9); as noted above, this can be seen in the form of the "washing" jets seen with bileaflet valves (Fig. 19.13b, Video 19.9). Minor regurgitant jets are also seen with biologic valves, including THVs. Pathologic regurgitation—characterized by one or more prominent areas of color flow Doppler regurgitation—can be either central or paravalvu-

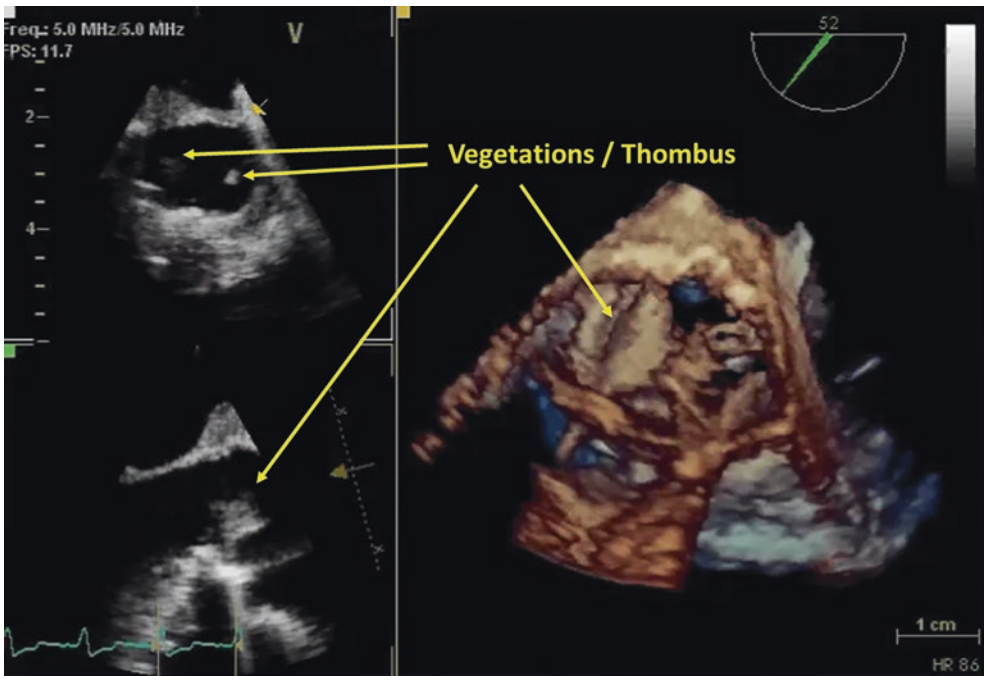

Fig. 19.18 Vegetation and thrombus formation in a bioprosthetic aortic valve using 2D/3D imaging. The patient presented with severe aortic valve stenosis related to infective endocarditis, with associated thrombus formation

lar (outside the valve sewing ring). Most pathologic central regurgitation is seen in biologic valves, but paravalvular regurgitation can be seen with both biologic and mechanical valves. The latter is seen as jets outside of the sewing ring of the prosthesis (Fig. 19.16, Video 19.12). It is not uncommon to see a small amount of paravalvular regurgitation immediately valve implantation (especially in THVs, see Fig. 19.11c). The degree of regurgitation can be estimated using the methods for quantification of native valvular regurgitation [82], although these can be more challenging with the shadowing and reverberations caused by the prosthetic valves (particularly mechanical valves). Commonly used parameters for semilunar valves include color flow Doppler jet width, vena contracta, pressure half-time, and diastolic flow reversal in the distal great artery; for AV valves, parameters include vena contracta, color flow Doppler jet area, as well as reversal of flow in the pulmonary or systemic veins for AV valves. A discussion of this evaluation is given in Chaps. 9 and 13. Regardless of valve type and position, when pathologic regurgitation is suspected, a careful evaluation must be made as to possible etiology. This includes location of the regurgitation (central vs. paravalvular), and possible mechanism or regurgitation (leaflet dysfunction, improper valve size/geometric mismatch, valve dehiscence, etc.).

When evaluating antegrade flow across prosthetic valves, it is important to remember that the flow characteristics and velocities across prosthetic valves (particularly mechanical valves) will often differ from comparably sized native valves. In general, the spectral Doppler velocities across these valves tend to be higher. As mentioned above, several studies have presented expected Doppler velocities, gradients and effective orifice area for a wide range of biologic and mechanical aortic and mitral valves [62, 84, 85]. Tables 19.4a and 19.4b show representative data abstracted from one of these studies [84] for several common prosthetic aortic and mitral valves. It should be noted that the labeled valve "size" (e.g. 21, 23 mm) represents the outer valve diameter in millimeters as given by the manufacturer. However, this diameter by itself is not useful, because the flow characteristics and cross-sectional area between two identically sized valves might be completely different. Hence the effective orifice area (EOA) presented in these tables represents a better parameter for valve comparisons and overall prosthetic valve evaluation; it is an important parameter utilized in adult patients for clinical prosthetic valve assessment. The EOA is analogous to valve orifice area for a native valve, and is calculated in the same manner by the continuity equation (Chap. 1):

- EOA = Stroke volume/VTI_{PrV}
- VTI_{PrV} = Velocity time integral (VTI) through the prosthesis, measured by continuous wave Doppler
- Stroke volume = VTI of the left ventricular outflow tract (by pulsed wave Doppler) multiplied by the left ventricular outflow tract cross sectional area (with prosthetic mitral valves, the calculated stroke volume is valid assuming no significant aortic regurgitation exists).

The EOA is generally a better index of valve function than gradient alone, because it is will not vary with different flow states. An important concept for prosthetic valves is that the EOA must be appropriate for the flow requirements of the individual, otherwise *patient-prosthetic mismatch* (PPM) occurs. PPM is a term used to describe the clinical situation

Table 19.4a Doppler parameters across prosthetic aortic valves

Valve	Size (mm)	Peak gradient (mm Hg)	Mean gradient (mm Hg)	Peak velocity (m/s)	Effective orifice area (cm^2)
Stented bioprosthesis					
Hancock II (porcine)	21	20 ± 0.4	14.8 ± 4.1		1.23 ± 0.3
	23	24.7 ± 5.7	16.6 ± 6.9		1.39 ± 0.2
	25	20 ± 2	10.7 ± 3		1.47 ± 0.2
	27	14 ± 3			1.55 ± 0.2
	29	15 ± 3			1.6 ± 0.2
Mosaic (porcine)	21		12.4 ± 7.3		1.6 ± 0.7
	23		12.5 ± 7.4		2.1 ± 0.8
	25		10.1 ± 5.1		2.1 ± 1.6
	27		9.0		1.8 ± 0.4
	29		9.0		2.0 ± 0.4
Carpentier-Edwards (pericardial)	19	32.1 ± 3.4	24.2 ± 8.6	2.8 ± 0.1	
	21	25.7 ± 9.9	20.3 ± 9.1	2.6 ± 0.4	1.2 ± 0.3
	23	21.7 ± 8.6	13.0 ± 5.3	2.3 ± 0.5	1.5 ± 0.4
	25	16.5 ± 5.4	9.0 ± 2.3	2.0 ± 0.3	1.8 ± 0.3
	27	19.2 ± 0	5.6	1.6	2.1 ± 0.4
	29	17.6 ± 0	11.6	2.1	2.2 ± 0.4
Mitroflow (pericardial)	19	18.7 ± 5.1	10.3 ± 3		1.1 ± 0.1
	21	20.2	15.4	2.3	1.3 ± 0.1
	23	14.0 ± 4.9	7.6 ± 3.4	1.9 ± 0.3	1.5 ± 0.2
	25	17 ± 11.3	10.8 ± 6.5	2 ± 0.7	1.8 ± 0.2
	27	13 ± 3	6.6 ± 1.7	1.8 ± 0.2	
Stentless bioprosthesis					
Medtronic Freestyle	19		13.0		
	21		8 ± 2.6		1.6 ± 0.3
	23		7.2 ± 2.5		1.9 ± 0.5
	25		5.4 ± 1.5		2.0 ± 0.4
	27		4.7 ± 1.6		2.5 ± 0.5
St Jude Toronto SPV	21	18.6 ± 11.8	7.6 ± 4.4		1.2 ± 0.7
	23	13.6 ± 7.3	7.1 ± 4.3		1.6 ± 0.8
	25	12.2 ± 5.8	6.2 ± 3.1		1.6 ± 0.4
	27	10 ± 4.6	4.8 ± 2.3		2 ± 0.4
	29	7.9 ± 4.2	3.9 ± 2.2		2.4 ± 0.7
Mechanical					
Medtronic-Hall	20	34.4 ± 13.1	17.1 ± 5.3	2.9 ± 0.4	1.21 ± 0.45
	21	26.9 ± 10.5	14.1 ± 5.9	2.4 ± 0.4	1.08 ± 0.17
	23	26.9 ± 8.9	13.5 ± 4.8	2.4 ± 0.6	1.36 ± 0.39
	25	17.1 ± 7.0	9.5 ± 4.3	2.3 ± 0.5	1.9 ± 0.47
	27	18.7 ± 9.7	8.7 ± 5.6	2.1 ± 0.5	1.9 ± 0.16
	29			1.6	
Carbomedics (bileaflet)	17	33.4 ± 13.2	20.1 ± 7.1	—	1.02 ± 0.2
	19	33.3 ± 11.2	11.6 ± 5.1	3.1 ± 0.4	1.25 ± 0.4
	21	26.3 ± 10.3	12.7 ± 4.3	2.6 ± 0.5	1.42 ± 0.4
	23	24.6 ± 6.9	11.3 ± 3.8	2.4 ± 0.4	1.69 ± 0.3
	25	20.3 ± 8.7	9.3 ± 4.7	2.3 ± 0.3	2.04 ± 0.4
	27	19.1 ± 7.0	8.4 ± 2.8	2.2 ± 0.4	2.55 ± 0.3
	29	12.5 ± 4.7	5.8 ± 3.2	1.9 ± 0.3	2.63 ± 0.4
St Jude (bileaflet)	19	35.2 ± 11.2	19 ± 6.2	2.9 ± 0.5	1.01 ± 0.2
	21	28.3 ± 9.9	15.8 ± 5.7	2.6 ± 0.5	1.33 ± 0.3
	23	25.3 ± 7.9	13.8 ± 5.3	2.6 ± 0.4	1.6 ± 0.4
	25	22.6 ± 7.7	12.7 ± 5.1	2.4 ± 0.5	1.93 ± 0.45
	27	19.9 ± 7.6	11.2 ± 4.8	2.2 ± 0.4	2.35 ± 0.6
	29	17.7 ± 6.4	9.9 ± 2.9	2 ± 0.1	2.81 ± 0.6
	31	16.0	10 ± 6	2.1 ± 0.6	3.08 ± 1.1

(Continued)

On-X (bileaflet)	19	21.3 ± 10.8	11.8 ± 3.4	—	1.5 ± 0.2
	21	16.4 ± 5.9	9.9 ± 3.6	—	1.7 ± 0.4
	23	15.9 ± 6.4	8.5 ± 3.3	—	2.0 ± 0.6
	25	16.5 ± 10.2	9 ± 5.3	—	2.4 ± 0.8
	27-29	11.4 ± 4.6	5.6 ± 2.7	—	3.2 ± 0.6
Starr-Edwards (Ball and Cage)	21	29			1.0
	23	32.6 ± 12.8	22 ± 8.8	4 ± 0	
	24	34.1 ± 10.3	22 ± 7.5	3.5 ± 0.5	1.1
	26	31.8 ± 9.0	19.7 ± 6.1	3.4 ± 0.5	
	27	30.8 ± 6.3	18.5 ± 3.7	3.2 ± 0.4	1.8
	29	29 ± 9.3	16.3 ± 5.5		

Table abstracted from *Rosenhek R,* et al. *Normal values for Doppler echocardiographic assessment of heart valve prostheses. J Am Soc Echocardiogr 2003;16:1116-27. With permission from Elsevier*

Table 19.4b Doppler parameters across prosthetic mitral valves

Valve	Size (mm)	Peak gradient (mm Hg)	Mean gradient (mm Hg)	Peak velocity (m/s)	Pressure half-time (ms)	Effective orifice area (cm^2)
Stented biologic						
Hancock II (porcine)	27					2.2 ± 0.14
	29					2.8 ± 0.11
	31					2.8 ± 0.1
	33					3.2 ± 0.2
Carpentier-Edwards (pericardial)	27		3.6	1.6		
	29		5.3 ± 3.4	1.7 ± 0.3		
	31		4 ± 0.8	1.5 ± 0.1		
	33		1.0	0.8		
Mitroflow (pericardial)	25		6.9	2.0	90	
	27		3.1 ± 0.9	2.5	90 ± 20	
	29		3.5 ± 1.7	1.4 ± 0.3	102 ± 21	
	31		3.9 ± 0.8	1.3 ± 0.3	91 ± 22	
Mechanical						
Carbomedics (bileaflet)	23			1.9 ± 0.1	126 ± 7	
	25	10.3 ± 2.3	3.6 ± 0.6	1.3 ± 0.1	93 ± 8	2.9 ± 0.8
	27	8.8 ± 3.5	3.5 ± 1.0	1.6 ± 0.3	89 ± 20	2.9 ± 0.8
	29	8.8 ± 2.9	3.4 ± 1.0	1.5 ± 0.3	88 ± 17	2.3 ± 0.4
	31	8.9 ± 2.3	3.3 ± 0.9	1.6 ± 0.3	92 ± 24	2.8 ± 1.1
	33	8.8 ± 2.2	4.8 ± 2.5	1.5 ± 0.2	93 ± 12	
St Jude (bileaflet)	23		4	1.5	160	1.0
	25		2.5 ± 1	1.3 ± 1.2	75 ± 4	1.4 ± 0.2
	27	11 ± 4	5 ± 1.8	1.6 ± 0.3	75 ± 10	1.7 ± 0.2
	29	10 ± 3	4.2 ± 1.8	1.6 ± 0.3	85 ± 10	1.8 ± 0.2
	31	12 ± 6	4.5 ± 2.2	1.6 ± 0.3	74 ± 13	2.0 ± 0.3
On-X (bileaflet)	25	11.5 ± 3.2	5.3 ± 2.1			1.9 ± 1.1
	27-29	10.3 ± 4.5	4.5 ± 1.6			2.2 ± 0.5
	31-33	9.8 ± 3.8	4.8 ± 2.4			2.5 ± 1.1
Starr-Edwards (Ball and Cage)	26		10			
	28		7 ± 2.8			
	30	12.2 ± 4.6	7 ± 2.5	1.7 ± 0.3	125 ± 25	1.7 ± 0.4
	32	11.5 ± 4.2	5.1 ± 2.5	1.7 ± 0.3	110 ± 25	2 ± 0.4
	34		5			

Table abstracted from *Rosenhek R,* et al. *Normal values for Doppler echocardiographic assessment of heart valve prostheses. J Am Soc Echocardiogr 2003;16:1116-27. With permission from Elsevier*

when the EOA of a prosthetic valve is too small in relation to a patient's body size, resulting in abnormally high postoperative gradients [62, 86]. Studies in adults have shown that aortic PPM is associated with worsening symptoms and impaired exercise capacity, as well as adverse cardiac events and long-term mortality [87–90]; mitral PPM is associated with persisting pulmonary hypertension and increased CHF as well as reduced survival [91]. When indexed to body sur-

Table 19.5 Threshold values of indexed prosthetic valve effective orifice area (EOA) for the identification and quantification of prosthesis-patient mismatch

	Mild or not clinically significant cm^2/m^2	Moderate cm^2/m^2	Severe cm^2/m^2
Aortic position	>0.85 (0.8–0.9)	≤0.85 (0.8–0.9)	≤0.65 (0.6–0.7)
Mitral position	>1.2 (1.2–1.3)	≤1.2 (1.2–1.3)	≤0.9 (0.9)

Numbers in parentheses represent the range of threshold values that have been used in the literature

From Pibarot and Dumesnil, Prosthetic Heart Valves: Selection of the Optimal Prosthesis and Long-Term Management. Circulation 2009; 119(7):1034-1048. Used with permission of Walters-Kluwer

face area, the EOA is the only parameter found to be consistently related to postoperative gradients and/or adverse clinical outcomes [92–94]. Table 19.5 shows threshold values for indexed EOA generally used to identify and quantify the severity of PPM in adults [62].

As noted above, the information from Tables 19.4a and 19.4b are derived from studies in which data were compiled from a number of adult studies. The tables are voluminous and comprehensive, and the reader is referred to these for further reference regarding other prosthetic valves. Nonetheless, from these data, some simplified general guidelines can be formulated to assist in the assessment of possible prosthetic aortic and mitral valve stenosis, and these are summarized by Zoghbi *et al.* [85] and presented in Table 19.5. These guidelines also utilize parameters such as Doppler velocity index (DVI) for prosthetic aortic valves, which is the ratio of velocities across the left ventricular outflow tract compared to the velocity across the prosthetic aortic valve, and the inverse relationship for mitral valves, the ratio of the prosthetic mitral valve VTI compared to the VTI across the left ventricular outflow tract. These dimensionless ratios—derived from the continuity equation—are much less dependent upon varying flow states. It should be noted that comparable data for prosthetic pulmonary and tricuspid valves is lacking, particularly regarding normal and abnormal EOAs and DVI/VTI. Therefore more general guidelines, also presented by Zoghbi et al., have been presented for these valves as follows [85]:

- *Findings suspicious for prosthetic pulmonary stenosis*
  - Cusp or leaflet thickening or immobility.
  - Narrowing of forward color map.
  - Peak velocity through the prosthesis >3 m/s or > 2 m/s through a homograft (suspicious but not diagnostic of stenosis).
  - Increase in peak velocity on serial studies (more reliable parameter).
  - Impaired right ventricular function or elevated right ventricular systolic pressure.
- *Findings suspicious for tricuspid valve stenosis*
  - Peak velocity > 1.7 m/s (because of respiratory variation, average ≥ 5 cycles).
  - Mean gradient ≥6 mm Hg (may be increased if there is valvular regurgitation).
  - Pressure half-time ≥ 230 ms.
  - Narrow inflow color map.
  - Nonspecific signs such as enlarged right atrium and engorged inferior vena cava.

In general, an integrated approach, using a combination of the criteria discussed above, works best when evaluating forward flow across any prosthetic valve.

For pediatric patients, there is a notable paucity of available published information regarding normal velocities and EOAs across prosthetic valves, particularly the smaller mitral and aortic valves. Much of the information used in this age group originates from adult data. Fortunately many of the same principles can still be applied, though comparable values to those obtained in adults are still lacking, and it is unclear whether certain parameters are equivalent in this population. For example, one study evaluating St. Jude and Carbomedics mitral prostheses in children found that peak early Doppler velocity—not EOA—correlated best with the manufacturer's geometric valve orifice area, and also pulmonary artery wedge pressure [95]. The use of the DVI and VTI ratios has not been established in the pediatric population. Also, PPM has not been evaluated closely in children, though it would seem evident that this particular concept has direct relevance in the pediatric population because of growth considerations. While the goal for valve replacement in children is to implant the largest possible prosthesis, patient growth will inevitably lead to some degree of PPM, even with a normally functioning prosthesis [85]. As noted above, the most widely accepted and validated parameter for identifying PPM in adult patients is the indexed EOA, and Table 19.6 shows threshold values for indexed EOA generally used to identify and quantify the severity of PPM in adults [62]. This table might also serve as useful guide in children, although the applicability of these values in pediatrics has yet to be fully determined.

For catheter-based implantable heart valves, the role of TEE will vary based upon the type of THV and its position. For TAVR (both SAPIEN and Evolut valves), TEE plays an integral role in all three phases of the procedure: preprocedural assessment of morphology and annular measurements, intraprocedural monitoring of all phases of the valve implantation (including guide wire and device positioning and valve deployment), and post-deployment assessment of possible paravalvar device leaks as well as ventricular function,

Table 19.6 Doppler parameters across prosthetic aortic and mitral valves

Parameter	Normal	Possible stenosis	Suggests significant stenosis
Aortic mechanical, stented valves			
Peak velocity (m/s)	<3	3–4	>4
Mean gradient (mm Hg)	<20	20–35	>35
DVI	≥0.30	0.29–0.25	<0.25
Effective Orifice Area (cm^2)	>1.2	1.2–0.8	<0.8
Contour of jet velocity through prosthetic aortic valve	Triangular, early peaking	Triangular to intermediate	Rounded, symmetrical contour
Acceleration time (ms)	<80	80–100	>100
Other pertinent findings: left ventricular size, function, hypertrophy			
Mitral valve prostheses			
Peak velocity (m/s)	<1.9	1.9	≥2.5
Mean gradient (mm Hg)	≤5	6–10	>10
VTI (PrMV)/VTI (LVOT)	<2.2	2.2–25	>2.5
Effective Orifice Area (cm^2)	≥2.0	1–2	<1
Pressure half-time (ms)	<130	130–200	>200
Other pertinent findings: left ventricular size and function, left atrial size, right ventricular size and function, estimation of pulmonary artery pressure			

DVI Doppler velocity index, equal to Velocity (Left ventricular outflow tract)/Velocity (Prosthetic aortic valve), *VTI* Velocity time integral, *PrMV* Prosthetic mitral valve, *LVOT* Left ventricular outflow tract

From: Zoghbi et al, Recommendations for evaluation of prosthetic valves with echocardiography and Doppler ultrasound. J Am Soc Echocardiogr 22(9): 975–1014, copyright 2009, with permission from Elsevier

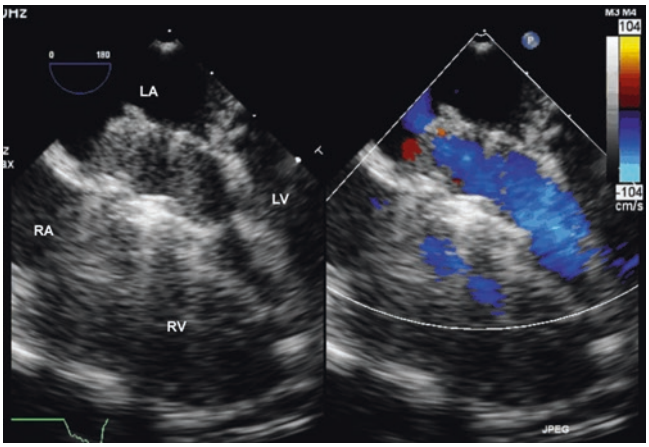

Fig. 19.19 Midesophageal four-chamber view using color compare of a mitral valve replacement with a Melody valve. There is unobstructed antegrade flow across the valve in diastole. There is shadowing produced by the Melody valve prosthesis. *LA* left atrium, *LV* left ventricle, *RA* right atrium, *RV* right ventricle

mitral valve assessment, pericardial effusion, aortic dissection, etc. [96, 97]. For Melody valve implantation, TEE is generally not performed during valve implantation, though transthoracic imaging is routinely obtained after the procedure to assess valve function and competence. For valve-in-valve implantation, the role of TEE will vary depending upon the fluoroscopic visibility of the biologic valve. In most cases, when a stented bioprosthesis is readily visible on fluoroscopy, TEE might not be necessary. However in those cases in which the bioprostheses is not readily visible (e.g. stentless), TEE might be helpful [70]. TEE can be very useful for evaluation of stented valves (such as the Melody) used as atrioventricular valve replacements [98–102] (Fig. 19.19 and Video 19.17).

Summary

This chapter reviews other applications of TEE including the critical care setting, when TEE is needed for better definition of the heart valves for infective endocarditis, thrombus evaluation in patients with strokes, and stenotic or regurgitant prosthetic valves. TEE provides added value when TTE has limited acoustic windows in critically ill patients.

Case-Based Examples

Case #1

Subject: 3 year old with aortic valve endocarditis

Clinical History: 3 year old previously healthy male who presented to an outside hospital with history of fever and flu-like symptoms. He became lethargic, was unable to move his right side and was found to have nuchal rigidity. Evaluation included a lumbar puncture, blood cultures were obtained and he was started on antibiotics. A head CT showed a left middle cerebral artery stroke with an acute and subacute left parietal infarct and thrombus formation. His blood cultures grew *Staphylococcus aureus* and a TTE showed a large mass in his aortic valve with fibrinous strands. He was transferred to our hospital for further management of the embolic stroke related

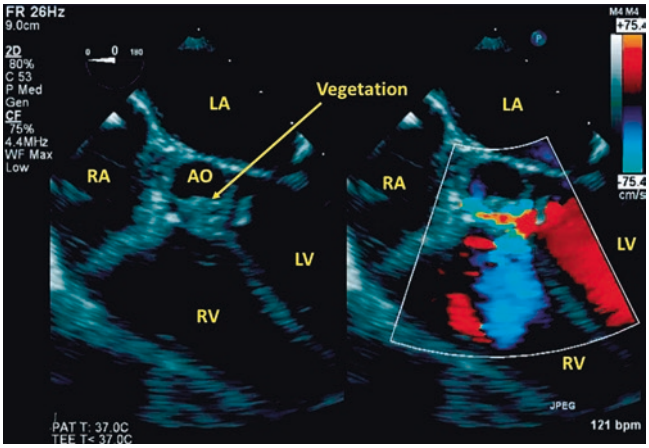

Fig. 19.20 **Case #1.** Vegetation is seen on the aortic valve from endocarditis in the midesophageal five-chamber view. There is a ventricular septal defect that occurred as a complication of the endocarditis, and color Doppler shows flow across the defect. *AO* aorta, *LA* left atrium, *LV* left ventricle, *RA* right atrium, *RV* right ventricle

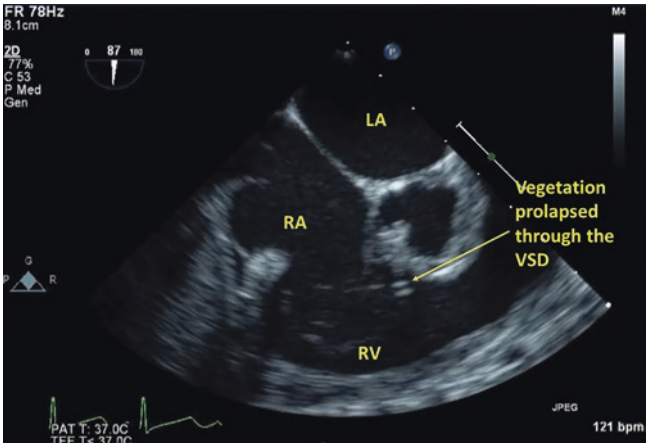

Fig. 19.22 **Case #1.** The patient from Fig. 19.20, again using a modified midesophageal right ventricular inflow-outflow view with a transducer angle of 87°. The vegetation has prolapsed through the aortic valve across the ventricular septal defect (VSD). *LA* left atrium, *RA* right atrium, *RV* right ventricle

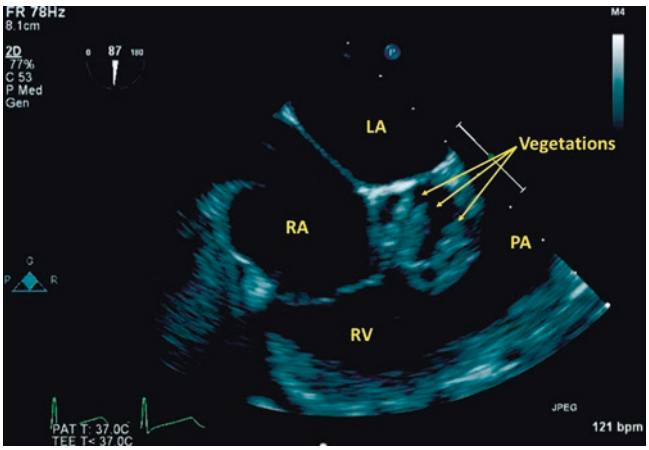

Fig. 19.21 **Case #1.** Multiple vegetations are seen on the aortic valve in a modified midesophageal right ventricular inflow-outflow view with a transducer angle of 87°. *LA* left atrium, *PA* pulmonary artery, *RA* right atrium, *RV* right ventricle

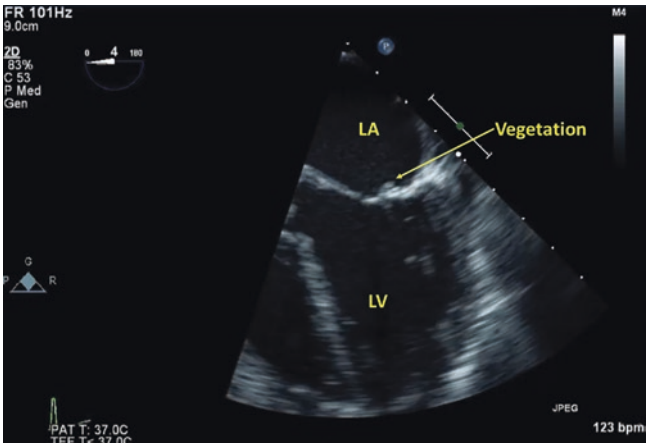

Fig. 19.23 **Case #1.** Midesophageal four-chamber view. Vegetation on the mitral valve. *LA* left atrium, *LV* left ventricle

to his IE. Two weeks later, he was taken to the operating room for debridement of the aortic vegetation. Intraoperative TEE was performed as a preoperative examination.

TEE Findings:

Figure 19.20, Video 19.18: A vegetation is seen on the aortic valve in the midesophageal five-chamber view. There is a ventricular septal defect that occurred as a complication of the endocarditis, and color Doppler shows flow across the defect.

Figure 19.21, Video 19.19: Multiple vegetations are seen on the aortic valve in a modified midesophageal right ventricular inflow-outflow view with a transducer angle of 87°.

Figure 19.22, Video 19.20: Again using a modified midesophageal right ventricular inflow-outflow view with a transducer angle of 87°. The vegetation has prolapsed through the aortic valve across the ventricular septal defect.

Figure 19.23, Video 19.21: Midesophageal fourMidesophageal four-chamber view. Vegetation on the mitral valve.

Figure 19.24, Video 19.22: Midesophageal four-chamber view. Vegetation on the tricuspid valve

Figure 19.25, Videos 19.23 and 19.24: Sinus of Valsalva aneurysm formation from infective endocarditis, as seen from a color compare image of a midesophageal aortic valve long axis view. There is a prominent vegetation noted adjacent to the aneurysm. Color Doppler shows that there is left to right shunting across a ventricular septal defect (VSD). LA, left atrium; LV, left ventricle; RV, right ventricle.

Discussion: This case illustrates the destructive nature of infective endocarditis (IE). The infectious process has damaged the aortic sinus of Valsalva and created a ventricular

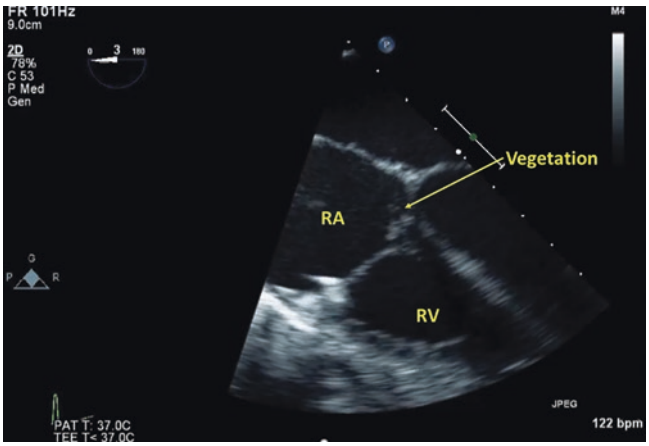

Fig. 19.24 **Case #1.** Midesophageal four-chamber view. Vegetation on the tricuspid valve. *RA* right atrium, *RV* right ventricle

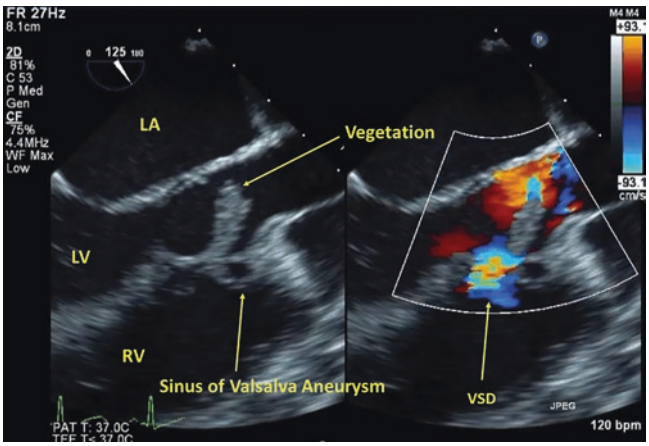

Fig. 19.25 **Case #1.** Sinus of Valsalva aneurysm formation from infective endocarditis, as seen from a color compare image of a midesophageal aortic valve long axis view. Color Doppler shows that there is left to right shunting across a ventricular septal defect (VSD). *LA* left atrium, *LV* left ventricle, *RV* right ventricle, *VSD* ventricular septal defect

septal defect. TEE was useful for visualization of the infective endocarditis.

Case #2

Subject: 17 year old with dilated cardiomyopathy, LV thrombus.

Clinical History: 17 year old with dilated cardiomyopathy, undergoing ventricular assist device placement (TEE done at that time).

TEE Findings:
Figure 19.26, Video 19.25: TEE showed a possible thrombus; however, it was unclear whether it might be a prominent papillary muscle. Thrombus was confirmed at time of Heart Mate™ ventricular assist device placement

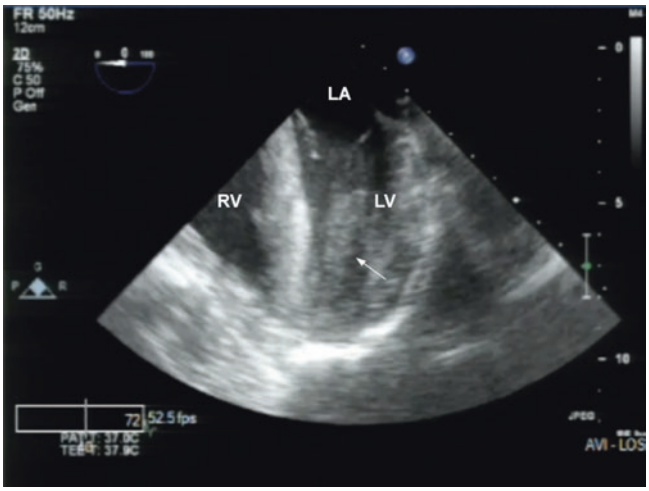

Fig. 19.26 **Case #2.** Left ventricular (LV) thrombus (arrow) in a patient with dilated cardiomyopathy, undergoing ventricular assist device placement. *LA* left atrium, *LV* left ventricle. Vegetation and thrombus formation in a bioprosthetic valve using 2D/3D imaging

Discussion: This case shows how TEE can demonstrate the presence of intracardiac thrombus, and this is important information for a number of different clinical settings, as discussed above.

Questions and Answers

1. Which of the following is a *major* Duke criterion for the diagnosis of infective endocarditis?
   a. Osler's nodes
   b. Fever >38 ° C.
   c. Oscillating mass noted on a valve as noted by echocardiography
   d. High-risk predisposing cardiac condition such as rheumatic heart disease

Answer: c

Explanation: The Duke criteria incorporate clinical, laboratory, pathologic, and echocardiographic criteria. They are subdivided into major and minor criteria. Major criteria include two separate blood cultures positive for typical organisms that cause endocarditis (e.g. *Staphylococcus aureus*, Viridans strepotocci), and echocardiographic features typical for endocarditis including an oscillating intracardiac mass (vegetation), abscess, or new/partial dehiscence of a prosthetic valve. Osler's nodes (an immunologic phenomenon), fever >38 °C, and high risk-cardiac conditions are all minor Duke criteria.

2. Of the following, which is the most common causative organism for infective endocarditis in children?
   a. *Staphylococcus aureus*
   b. *Neisseria meningitidis*
   c. *Streptococcus pneumoniae*
   d. *Hemophilus influenzae*

Answer: a

Explanation: *Staphylococcus aureus and* Viridans streptococci are by far the dominant organisms causing endocarditis in children. The other organisms mentioned, while responsible for other childhood illnesses, do not have a high association with infective endocarditis.

3. All of the following are known echocardiographic manifestations of IE *except*:
   a. Abscesses
   b. Flail valve leaflets
   c. Dehiscence of a prosthetic valve
   d. Appearance of left ventricular noncompaction

Answer: d

Explanation. From an echocardiographic standpoint, IE can present in a number of different ways, including oscillating masses adherent to the valves (vegetations), abscesses, fistulous tracks, valve disruption (flail leaflets), and dehiscence of a prosthetic valve. Left ventricular compaction is an echocardiographic appearance of abnormal left ventricular myocardial anatomy (and sometimes function), and it is not a known manifestation of IE.

4. Which of the following predisposes to thrombus formation in the left atrial appendage:
   a. Aortic regurgitation
   b. Mitral regurgitation
   c. Atrial fibrillation
   d. Ebstein's anomaly of the tricuspid valve

Answer: c

Explanation: Those patients with discoordinated atrial contraction, resulting in stasis of atrial blood flow, can be predisposed to development of thrombus in the left atrial appendage. This is seen in patients who have atrial fibrillation/flutter. The other three choices still have coordinated atrial contraction, although if atrial dilation form mitral stenosis/mitral regurgitation is severe enough, atrial fibrillation could occur.

5. All of the following regarding the echocardiographic evaluation of a mechanical bileaflet tilting disc valves are true *except*:
   a. Acoustic shadowing can interfere with visualization of the valve
   b. It is abnormal to see any systolic regurgitant jets with a mechanical valve
   c. Spectral Doppler velocities will be different than a native valve
   d. It is abnormal to see a paravalvar regurgitant jet outside the sewing ring of the valve

Answer: b

Explanation: When a mechanical valve is closed, there are normally characteristic regurgitant ("washing") jets that can be seen at the pivot points of the valve, angled centrally. These are a normal part of the valve design. On the other hand, it is abnormal to see a paravalvar regurgitant jet outside the sewing ring of the valve. The other two choices are accurate: acoustic shadowing can interfere with visualization of the valve, and spectral Doppler velocities across the mechanical valve tend to be higher than those of a native valve.

References

1. Baltimore RS, Gewitz M, Baddour LM, Beerman LB, Jackson MA, Lockhart PB, et al. Infective endocarditis in childhood: 2015 update: a scientific statement from the American Heart Association. Circulation. 2015;132(15):1487–515.
2. Bayer AS, Bolger AF, Taubert KA, Wilson W, Steckelberg J, Karchmer AW, et al. Diagnosis and management of infective endocarditis and its complications. Circulation. 1998;98(25):2936–48.
3. Ferrieri P, Gewitz MH, Gerber MA, Newburger JW, Dajani AS, Shulman ST, et al. Unique features of infective endocarditis in childhood. Circulation. 2002;105(17):2115–26.
4. Elder RW, Baltimore RS. The changing epidemiology of pediatric endocarditis. Infect Dis Clin N Am. 2015;29(3):513–24.
5. Saiman L, Prince A, Gersony WM. Pediatric infective endocarditis in the modern era. J Pediatr. 1993;122(6):847–53.
6. Morris CD, Reller MD, Menashe VD. Thirty-year incidence of infective endocarditis after surgery for congenital heart defect. JAMA. 1998;279(8):599–603.
7. Martin JM, Neches WH, Wald ER. Infective endocarditis: 35 years of experience at a children's hospital. Clin Infect Dis. 1997;24(4):669–75.
8. Lin YT, Hsieh KS, Chen YS, Huang IF, Cheng MF. Infective endocarditis in children without underlying heart disease. J Microbiol Immunol Infect. 2013;46(2):121–8.
9. Stockheim JA, Chadwick EG, Kessler S, Amer M, Abdel-Haq N, Dajani AS, et al. Are the Duke criteria superior to the Beth Israel criteria for the diagnosis of infective endocarditis in children? Clin Infect Dis. 1998;27(6):1451–6.
10. Li JS, Sexton DJ, Mick N, Nettles R, Fowler VG Jr, Ryan T, et al. Proposed modifications to the Duke criteria for the diagnosis of infective endocarditis. Clin Infect Dis. 2000;30(4):633–8.
11. Roe MT, Abramson MA, Li J, Heinle SK, Kisslo J, Corey GR, et al. Clinical information determines the impact of transesophageal echocardiography on the diagnosis of infective endocarditis by the duke criteria. Am Heart J. 2000;139(6):945–51.
12. Rohmann S, Erbel R, Mohr-Kahaly S, Meyer J. Use of transoesophageal echocardiography in the diagnosis of abscess in infective endocarditis. Eur Heart J. 1995;16(Suppl B):54–62.
13. Rohmann S, Erbel R, Gorge G, Makowski T, Mohr-Kahaly S, Nixdorff U, et al. Clinical relevance of vegetation localization by

transoesophageal echocardiography in infective endocarditis. Eur Heart J. 1992;13(4):446–52.
14. Rohmann S, Seifert T, Erbel R, Jakob H, Mohr-Kahaly S, Makowski T, et al. Identification of abscess formation in native-valve infective endocarditis using transesophageal echocardiography: implications for surgical treatment. Thorac Cardiovasc Surg. 1991;39(5):273–80.
15. Erbel R, Rohmann S, Drexler M, Mohr-Kahaly S, Gerharz CD, Iversen S, et al. Improved diagnostic value of echocardiography in patients with infective endocarditis by transoesophageal approach. A prospective study. Eur Heart J. 1988;9(1):43–53.
16. Klodas E, Edwards WD, Khandheria BK. Use of transesophageal echocardiography for improving detection of valvular vegetations in subacute bacterial endocarditis. J Am Soc Echocardiogr. 1989;2(6):386–9.
17. Daniel WG, Mugge A, Martin RP, Lindert O, Hausmann D, Nonnast-Daniel B, et al. Improvement in the diagnosis of abscesses associated with endocarditis by transesophageal echocardiography. N Engl J Med. 1991;324(12):795–800.
18. Mugge A, Daniel WG, Frank G, Lichtlen PR. Echocardiography in infective endocarditis: reassessment of prognostic implications of vegetation size determined by the transthoracic and the transesophageal approach. J Am Coll Cardiol. 1989;14(3):631–8.
19. Reynolds HR, Jagen MA, Tunick PA, Kronzon I. Sensitivity of transthoracic versus transesophageal echocardiography for the detection of native valve vegetations in the modern era. J Am Soc Echocardiogr. 2003;16(1):67–70.
20. Daniel WG, Mugge A, Grote J, Hausmann D, Nikutta P, Laas J, et al. Comparison of transthoracic and transesophageal echocardiography for detection of abnormalities of prosthetic and bioprosthetic valves in the mitral and aortic positions. Am J Cardiol. 1993;71(2):210–5.
21. Humpl T, McCrindle BW, Smallhorn JF. The relative roles of transthoracic compared with transesophageal echocardiography in children with suspected infective endocarditis. J Am Coll Cardiol. 2003;41(11):2068–71.
22. Penk JS, Webb CL, Shulman ST, Anderson EJ. Echocardiography in pediatric infective endocarditis. Pediatr Infect Dis J. 2011;30(12):1109–11.
23. Durack DT, Beeson PB. Experimental bacterial endocarditis. I. Colonization of a sterile vegetation. Br J Exp Pathol. 1972;53(1):44–9.
24. Durack DT, Beeson PB. Experimental bacterial endocarditis. II. Survival of a bacteria in endocardial vegetations. Br J Exp Pathol. 1972;53(1):50–3.
25. Karchmer AW. Infective endocarditis. In: Bonow RO, Mann DL, Zipes DP, Libby P, editors. Braunwald's heart disease: a textbook of cardiovascular medicine. 9th ed. Philadelphia, PA: Elsevier Saunders; 2012. p. 1540–60.
26. Zoghbi WA, Adams D, Bonow RO, Enriquez-Sarano M, Foster E, Grayburn PA, et al. Recommendations for noninvasive evaluation of native valvular regurgitation: a report from the American Society of Echocardiography Developed in Collaboration with the Society for Cardiovascular Magnetic Resonance. J Am Soc Echocardiogr. 2017;30(4):303–71.
27. Baddour LM, Wilson WR, Bayer AS, Fowler VG Jr, Tleyjeh IM, Rybak MJ, et al. Infective endocarditis in adults: diagnosis, antimicrobial therapy, and management of complications: a scientific statement for healthcare professionals from the American Heart Association. Circulation. 2015;132(15):1435–86.
28. Shaffer EM, Snider AR, Beekman RH, Behrendt DM, Peschiera AW. Sinus of Valsalva aneurysm complicating bacterial endocarditis in an infant: diagnosis with two-dimensional and Doppler echocardiography. J Am Coll Cardiol. 1987;9(3):588–91.
29. Anguera I, Miro JM, Vilacosta I, Almirante B, Anguita M, Munoz P, et al. Aorto-cavitary fistulous tract formation in infective endocarditis: clinical and echocardiographic features of 76 cases and risk factors for mortality. Eur Heart J. 2005;26(3):288–97.
30. Anguera I, Miro JM, San Roman JA, de Alarcon A, Anguita M, Almirante B, et al. Periannular complications in infective endocarditis involving prosthetic aortic valves. Am J Cardiol. 2006;98(9):1261–8.
31. Sievers HH, Stierle U, Charitos EI, Hanke T, Misfeld M, Matthias Bechtel JF, et al. Major adverse cardiac and cerebrovascular events after the Ross procedure: a report from the German-Dutch Ross Registry. Circulation. 2010;122(11 Suppl):S216–23.
32. Hasbun R, Vikram HR, Barakat LA, Buenconsejo J, Quagliarello VJ. Complicated left-sided native valve endocarditis in adults: risk classification for mortality. JAMA. 2003;289(15):1933–40.
33. Mills J, Utley J, Abbott J. Heart failure in infective endocarditis: predisposing factors, course, and treatment. Chest. 1974;66(2):151–7.
34. Ryan EW, Bolger AF. Transesophageal echocardiography (TEE) in the evaluation of infective endocarditis. In: Foster E, editor. Cardiology clinics: Transesophageal Echocardiography. Division of Cardiology, Department of Medicine, University of California, San Francisco, USA; 2000. p. 773–87.
35. Prendergast BD, Tornos P. Surgery for infective endocarditis: who and when? Circulation. 2010;121(9):1141–52.
36. Saiman L, Prince A, Gersony WM. Pediatric infective endocarditis in the modern era. J Pediatr. 1993;122(6):847–53.
37. Baddour LM, Wilson WR, Bayer AS, Fowler VGJ, Bolger AF, Levison ME, et al. Infective endocarditis: diagnosis, antimicrobial therapy, and management of complications: a statement for healthcare professionals from the Committee on Rheumatic Fever, Endocarditis, and Kawasaki Disease, Council on Cardiovascular Disease in the Young, and the Councils on Clinical Cardiology, Stroke, and Cardiovascular Surgery and Anesthesia, American Heart Association: endorsed by the Infectious Diseases Society of America. Circulation. 2005;111(23):e394–434.
38. Lopez JA, Ross RS, Fishbein MC, Siegel RJ. Nonbacterial thrombotic endocarditis: a review. Am Heart J. 1987;113(3):773–84.
39. Asopa S, Patel A, Khan OA, Sharma R, Ohri SK. Non-bacterial thrombotic endocarditis. Eur J Cardiothorac Surg. 2007;32(5):696–701.
40. González Quintela A, Candela MJ, Vidal C, Román J, Aramburo P. Non-bacterial thrombotic endocarditis in cancer patients. Acta Cardiol. 1991;46(1):1–9.
41. Beynon RP, Bahl VK, Prendergast BD. Infective endocarditis. BMJ. 2006;333(7563):334–9.
42. Agmon Y, Khandheria BK, Gentile F, Seward JB. Echocardiographic assessment of the left atrial appendage. J Am Coll Cardiol. 1999;34(7):1867–77.
43. Stabile G, Russo V, Rapacciuolo A, De Divitiis M, De Simone A, Solimene F, et al. Transesophageal echocardiograpy in patients with persistent atrial fibrillation undergoing electrical cardioversion on new oral anticoagulants: a multi center registry. Int J Cardiol. 2015;184:283–4.
44. de Divitiis M, Omran H, Rabahieh R, Rang B, Illien S, Schimpf R, et al. Right atrial appendage thrombosis in atrial fibrillation: its frequency and its clinical predictors. Am J Cardiol. 1999;84(9):1023–8.
45. Ozer O, Sari I, Davutoglu V. Right atrial appendage: forgotten part of the heart in atrial fibrillation. Clin Appl Thromb Hemost. 2010;16(2):218–20.
46. Schweizer P, Bardos P, Erbel R, Meyer J, Merx W, Messmer BJ, et al. Detection of left atrial thrombi by echocardiography. Br Heart J. 1981;45(2):148–56.
47. Aschenberg W, Schluter M, Kremer P, Schroder E, Siglow V, Bleifeld W. Transesophageal two-dimensional echocardiography for the detection of left atrial appendage thrombus. J Am Coll Cardiol. 1986;7(1):163–6.
48. Manning WJ, Weintraub RM, Waksmonski CA, Haering JM, Rooney PS, Maslow AD, et al. Accuracy of transesophageal echo-

cardiography for identifying left atrial thrombi. A prospective, intraoperative study. Ann Intern Med. 1995;123(11):817–22.
49. Veinot JP, Harrity PJ, Gentile F, Khandheria BK, Bailey KR, Eickholt JT, et al. Anatomy of the normal left atrial appendage: a quantitative study of age-related changes in 500 autopsy hearts: implications for echocardiographic examination. Circulation. 1997;96(9):3112–5.
50. Karakus G, Kodali V, Inamdar V, Nanda NC, Suwanjutah T, Pothineni KR. Comparative assessment of left atrial appendage by transesophageal and combined two- and three-dimensional transthoracic echocardiography. Echocardiography. 2008;25(8):918–24.
51. Werner JA, Cheitlin MD, Gross BW, Speck SM, Ivey TD. Echocardiographic appearance of the Chiari network: differentiation from right-heart pathology. Circulation. 1981;63(5):1104–9.
52. Zoghbi WA, Chambers JB, Dumesnil JG, Foster E, Gottdiener JS, Grayburn PA, et al. Recommendations for evaluation of prosthetic valves with echocardiography and doppler ultrasound: a report from the American Society of Echocardiography's Guidelines and Standards Committee and the Task Force on Prosthetic Valves, developed in conjunction with the American College of Cardiology Cardiovascular Imaging Committee, Cardiac Imaging Committee of the American Heart Association, the European Association of Echocardiography, a registered branch of the European Society of Cardiology, the Japanese Society of Echocardiography and the Canadian Society of Echocardiography, endorsed by the American College of Cardiology Foundation, American Heart Association, European Association of Echocardiography, a registered branch of the European Society of Cardiology, the Japanese Society of Echocardiography, and Canadian Society of Echocardiography. J Am Soc Echocardiogr. 2009;22(9):975–1014; quiz 82–4.
53. Ross DN. Replacement of aortic and mitral valves with a pulmonary autograft. Lancet. 1967;2(7523):956–8.
54. Chambers JC, Somerville J, Stone S, Ross DN. Pulmonary autograft procedure for aortic valve disease: long-term results of the pioneer series. Circulation. 1997;96(7):2206–14.
55. Athanasiou T, Cherian A, Ross D. The Ross II procedure: pulmonary autograft in the mitral position. Ann Thorac Surg. 2004;78(4):1489–95.
56. Protopapas AD, Athanasiou T. Contegra conduit for reconstruction of the right ventricular outflow tract: a review of published early and mid-time results. J Cardiothorac Surg. 2008;3:62.
57. Hickey EJ, McCrindle BW, Blackstone EH, Yeh T, Pigula F, Clarke D, et al. Jugular venous valved conduit (Contegra) matches allograft performance in infant truncus arteriosus repair. Eur J Cardiothorac Surg. 2008;33(5):890–8.
58. Christenson JT, Sierra J, Colina Manzano NE, Jolou J, Beghetti M, Kalangos A. Homografts and xenografts for right ventricular outflow tract reconstruction: long-term results. Ann Thorac Surg. 2010;90(4):1287–93.
59. Dave H, Mueggler O, Comber M, Enodien B, Nikolaou G, Bauersfeld U, et al. Risk factor analysis of 170 single-institutional contegra implantations in pulmonary position. Ann Thorac Surg. 2011;91(1):195–302; discussion 202–3.
60. Prog Pediatr Cardiol. In: Hopkins RA, editor. Tissue and bioengineering for congenital cardiac disease 2006. p. 137–244.
61. Aslam AK, Aslam AF, Vasavada BC, Khan IA. Prosthetic heart valves: types and echocardiographic evaluation. Int J Cardiol. 2007;122(2):99–110.
62. Pibarot P, Dumesnil JG. Prosthetic heart valves: selection of the optimal prosthesis and long-term management. Circulation. 2009;119(7):1034–48.
63. Oosterhof T, Hazekamp MG, Mulder BJM. Opportunities in pulmonary valve replacement. Expert Rev Cardiovasc Ther. 2009;7(9):1117–22.
64. Kidane AG, Burriesci G, Cornejo P, Dooley A, Sarkar S, Bonhoeffer P, et al. Current developments and future prospects for heart valve replacement therapy. J Biomed Mater Res B Appl Biomater. 2009;88(1):290–303.
65. Bonow RO, Carabello BA, Chatterjee K, de Leon AC, Faxon DP, Freed MD, et al. 2008 Focused update incorporated into the ACC/AHA 2006 guidelines for the management of patients with valvular heart disease: a report of the American College of Cardiology/American Heart Association Task Force on Practice Guidelines (Writing Committee to Revise the 1998 Guidelines for the Management of Patients With Valvular Heart Disease): endorsed by the Society of Cardiovascular Anesthesiologists, Society for Cardiovascular Angiography and Interventions, and Society of Thoracic Surgeons. Circulation. 2008;118(15):e523–661.
66. Waterbolk TW, Hoendermis ES, den Hamer IJ, Ebels T. Pulmonary valve replacement with a mechanical prosthesis. Promising results of 28 procedures in patients with congenital heart disease. Eur J Cardiothorac Surg. 2006;30(1):28–32.
67. Fleming GA, Hill KD, Green AS, Rhodes JF. Percutaneous pulmonary valve replacement. Prog Pediatr Cardiol. 2012;33(2):143–50.
68. Momenah TS, El Oakley R, Al Najashi K, Khoshhal S, Al Qethamy H, Bonhoeffer P. Extended application of percutaneous pulmonary valve implantation. J Am Coll Cardiol. 2009;53(20):1859–63.
69. Hasan BS, McElhinney DB, Brown DW, Cheatham JP, Vincent JA, Hellenbrand WE, et al. Short-term performance of the transcatheter Melody valve in high-pressure hemodynamic environments in the pulmonary and systemic circulations. Circ Cardiovasc Interv. 2011;4(6):615–20.
70. Gurvitch R, Cheung A, Ye J, Wood DA, Willson AB, Toggweiler S, et al. Transcatheter valve-in-valve implantation for failed surgical bioprosthetic valves. J Am Coll Cardiol. 2011;58(21):2196–209.
71. Gillespie MJ, Dori Y, Harris MA, Sathanandam S, Glatz AC, Rome JJ. Bilateral branch pulmonary artery melody valve implantation for treatment of complex right ventricular outflow tract dysfunction in a high-risk patient. Circ Cardiovasc Interv. 2011;4(4):e21–3.
72. Billings FT, Kodali SK, Shanewise JS. Transcatheter aortic valve implantation: anesthetic considerations. Anesth Analg. 2009;108(5):1453–62.
73. Kenny D, Hijazi ZM, Kar S, Rhodes J, Mullen M, Makkar R, et al. Percutaneous implantation of the Edwards SAPIEN transcatheter heart valve for conduit failure in the pulmonary position: early phase 1 results from an international multicenter clinical trial. J Am Coll Cardiol. 2011;58(21):2248–56.
74. Rotman OM, Bianchi M, Ghosh RP, Kovarovic B, Bluestein D. Principles of TAVR valve design, modelling, and testing. Expert Rev Med Devices. 2018;15(11):771–91.
75. Siddique S, Gada H, Mumtaz MA, Vora AN. Should all low-risk patients now be considered for TAVR? Operative risk, clinical, and anatomic considerations. Curr Cardiol Rep. 2019;21(12):161.
76. Mankad SV, Aldea GS, Ho NM, Mankad R, Pislaru S, Rodriguez LL, et al. Transcatheter mitral valve implantation in degenerated bioprosthetic valves. J Am Soc Echocardiogr. 2018;31(8):845–59.
77. Pibarot P, Dumesnil JG. Prosthetic heart valves: selection of the optimal prosthesis and long-term management. Circulation. 2009;119(7):1034–48.
78. Rosenhek R, Binder T, Maurer G, Baumgartner H. Normal values for Doppler echocardiographic assessment of heart valve prostheses. J Am Soc Echocardiogr. 2003;16(11):1116–27.
79. Bach DS. Transesophageal echocardiographic (TEE) evaluation of prosthetic valves. Cardiol Clin. 2000;18(4):751–71.
80. Aslam AK, Aslam AF, Vasavada BC, Khan IA. Prosthetic heart valves: types and echocardiographic evaluation. Int J Cardiol. 2007;122(2):99–110.

81. Baumgartner H, Hung J, Bermejo J, Chambers JB, Evangelista A, Griffin BP, et al. Echocardiographic assessment of valve stenosis: EAE/ASE recommendations for clinical practice. J Am Soc Echocardiogr 2009;22(1):1–23; quiz 101–2.
82. Zoghbi WA, Enriquez-Sarano M, Foster E, Grayburn PA, Kraft CD, Levine RA, et al. Recommendations for evaluation of the severity of native valvular regurgitation with two-dimensional and Doppler echocardiography. J Am Soc Echocardiogr. 2003;16(7):777–802.
83. Quiñones M. Echocardiographic assessment of valve stenosis: EAE/ASE recommendations for clinical practice. J Am Soc Echocardiogr. 2009;22(1):1–23.
84. Rosenhek R, Binder T, Maurer G, Baumgartner H. Normal values for Doppler echocardiographic assessment of heart valve prostheses. J Am Soc Echocardiogr. 2003;16(11):1116–27.
85. Zoghbi WA, Chambers JB, Dumesnil JG, Foster E, Gottdiener JS, Grayburn PA, et al. Recommendations for evaluation of prosthetic valves with echocardiography and doppler ultrasound: a report From the American Society of Echocardiography's Guidelines and Standards Committee and the Task Force on Prosthetic Valves, developed in conjunction with the American College of Cardiology Cardiovascular Imaging Committee, Cardiac Imaging Committee of the American Heart Association, the European Association of Echocardiography, a registered branch of the European Society of Cardiology, the Japanese Society of Echocardiography and the Canadian Society of Echocardiography, endorsed by the American College of Cardiology Foundation, American Heart Association, European Association of Echocardiography, a registered branch of the European Society of Cardiology, the Japanese Society of Echocardiography, and Canadian Society of Echocardiography. J Am Soc Echocardiogr. 2009;22(9):975–1014; quiz 82–4.
86. Rahimtoola SH. The problem of valve prosthesis-patient mismatch. Circulation. 1978;58(1):20–4.
87. Pibarot P, Dumesnil JG. Hemodynamic and clinical impact of prosthesis-patient mismatch in the aortic valve position and its prevention. J Am Coll Cardiol. 2000;36(4):1131–41.
88. Mohty D, Mohty-Echahidi D, Malouf JF, Girard SE, Schaff HV, Grill DE, et al. Impact of prosthesis-patient mismatch on long-term survival in patients with small St Jude Medical mechanical prostheses in the aortic position. Circulation. 2006;113(3):420–6.
89. Walther T, Rastan A, Falk V, Lehmann S, Garbade J, Funkat AK, et al. Patient prosthesis mismatch affects short- and long-term outcomes after aortic valve replacement. Eur J Cardiothorac Surg. 2006;30(1):15–9.
90. Rahimtoola SH. Choice of prosthetic heart valve in adults an update. J Am Coll Cardiol. 2010;55(22):2413–26.
91. Lam B-K, Chan V, Hendry P, Ruel M, Masters R, Bedard P, et al. The impact of patient-prosthesis mismatch on late outcomes after mitral valve replacement. J Thorac Cardiovasc Surg. 2007;133(6):1464–73.
92. Blackstone EH, Cosgrove DM, Jamieson WRE, Birkmeyer NJ, Lemmer JH, Miller DC, et al. Prosthesis size and long-term survival after aortic valve replacement. J Thorac Cardiovasc Surg. 2003;126(3):783–96.
93. Koch CG, Khandwala F, Estafanous FG, Loop FD, Blackstone EH. Impact of prosthesis-patient size on functional recovery after aortic valve replacement. Circulation. 2005;111(24):3221–9.
94. Pibarot P, Dumesnil JG. Prosthesis-patient mismatch: definition, clinical impact, and prevention. Heart. 2006;92(8):1022–9.
95. Masuda M, Kado H, Tatewaki H, Shiokawa Y, Yasui H. Late results after mitral valve replacement with bileaflet mechanical prosthesis in children: evaluation of prosthesis-patient mismatch. Ann Thorac Surg. 2004;77(3):913–7.
96. Zamorano JL, Badano LP, Bruce C, Chan K-L, Gonçalves A, Hahn RT, et al. EAE/ASE recommendations for the use of echocardiography in new transcatheter interventions for valvular heart disease. J Am Soc Echocardiogr. 2011;24(9):937–65.
97. Holmes DR, Mack MJ, Kaul S, Agnihotri A, Alexander KP, Bailey SR, et al. 2012 ACCF/AATS/SCAI/STS expert consensus document on transcatheter aortic valve replacement. J Am Coll Cardiol. 2012;59(13):1200–54.
98. Shuto T, Kondo N, Dori Y, Koomalsingh KJ, Glatz AC, Rome JJ, et al. Percutaneous transvenous melody valve-in-ring procedure for mitral valve replacement. J Am Coll Cardiol. 2011;58(24):2475–80.
99. Kondo N, Shuto T, McGarvey JR, Koomalsingh KJ, Takebe M, Gorman RC, et al. Melody valve-in-ring procedure for mitral valve replacement: feasibility in four annuloplasty types. Ann Thorac Surg. 2012;93(3):783–8.
100. El-Eshmawi A, Love B, Bhatt HV, Pawale A, Boateng P, Adams DH. Direct access implantation of a Melody valve in native mitral valve: a hybrid approach in the presence of extensive mitral annular calcification. Ann Thorac Surg. 2015;99(3):1085.
101. Trezzi M, Cetrano E, Iacobelli R, Carotti A. Edwards Sapien 3 valve for mitral replacement in a child after melody valve endocarditis. Ann Thorac Surg. 2017;104(6):e429–e30.
102. Pluchinotta FR, Piekarski BL, Milani V, Kretschmar O, Burch PT, Hakami L, et al. Surgical atrioventricular valve replacement with melody valve in infants and children. Circ Cardiovasc Interv. 2018;11(11):e007145.